Analyzing force curves and image resolution for an AFM

Please check the document version of this publication:

• A submitted manuscript is the version of the article upon submission and before peer-review. There can be important differences between the submitted version and the official published version of record. People interested in the research are advised to contact the author for the final version of the publication, or visit the DOI to the publisher's website.
• The final author version and the galley proof are versions of the publication after peer review.
• The final published version features the final layout of the paper including the volume, issue and page numbers.

Link to publication

Analyzing force curves and image resolution for an AFM

Author: M.L. Bloo

Report no.: WPA 310053, February 1997

Report Trainee-ship Sept.-Dec. 1996

Professor: Prof. R.J. Hocken Ph.D., UNCC
             Prof.dr.ir. P.H.J. Schellekens, TUE

Advisor: J. Miller Ph.D., UNCC
             Ing. K.G. Struik, TUE

UNC Charlotte
Mechanical Engineering and
Engineering Science Department
Section Precision Engineering

TU Eindhoven
Mechanical Engineering Department
Production Technology and Automation
Section Precision Engineering

Summary

This report consists of two parts. The first part discusses the interactions, forces and deformation, taking place during measurements with an AFM (Atomic Force Microscope). In the beginning the mechanisms as well as the order of magnitude of the interactions are mentioned. This already shows that the order of magnitude of the contact forces, while measuring in air, will be larger than atomic forces. Then the interaction forces are investigated by looking at force curves made on several different samples (graphite, mica and gold). A force curve shows how the force is extended and retracted from the surface of the sample and most important it shows the size of the contact force while scanning. The ideal and real shape of force curves on these samples are discussed. The measured force curves all show an unexpected waving and slope in the extending and retracting stretch. In addition to the differences in shape between the ideal and real shape the accuracy and order of magnitude of the contact forces is discussed. It can be concluded that the accuracy is bad, because the stiffness of the cantilever is not know accurate. It is only known that the stiffness will be between the 0.09 and 0.51 N/m. There was no time to execute an experiment to determine the stiffness of the cantilever more accurate. Due to the 'unknown' cantilever stiffness only the order of magnitude of the measured contact forces can be discussed. It can be concluded that the order of magnitude of the contact forces (10^{-8}) is much larger than atomic forces (10^{-11}). Also the AFM re-engagement repeatability and the force curve repeatability became point of discussion. The repeatability of engagement is very satisfying, $\Delta x = 10$ nm and $\Delta y = 30$ nm, after taking in consideration some restrictions. Also the force curve repeatability seems to be satisfying, $2.8*10^{-8}$ N.

The second part of this report starts with discussing the difficulties concerning image interpretation. The points of interest discussed here are the vertical and lateral resolution, and the different difficulties with interpreting large scale or atomic scale images. After this theoretical introduction it is tried to find a relation between the image resolution and the contact force. Two experiments executed on graphite, mica and diamond samples are discussed. First for an hour a sample is imaged without changing the contact force, to see if imaging for a longer time already influences the resolution of the image. This influence is not noticed in the measurements. During executing the second experiment images are made while changing the contact force, to investigate the relationship searched for. While changing the contact force there are differences noticed in the images. For all the samples the lower limits of the contact force for measuring under ambient conditions is found.

Contents

Chapter 1

Introduction

1.1 Objective

In 1985 G. Binning, C. Gerber and C. Quate [5] invented the Atomic Force Microscope (AFM). It was discovered that a flexible cantilever with a very low spring-constant could be produced. With a cantilever that bent under smaller than interatomic forces, the topography of the sample could be measured without displacing the atoms. Several techniques for sensing the deflection of the cantilever have been investigated and developed. Originally, the tunneling current between the cantilever and another probe was used to sense the cantilever deflection, but eventually, interest focused on optical techniques. Most AFM's in use today rely on optical techniques to sense the cantilever deflection. The AFM relies on the precise scanning of the probe over the sample surface to reproduce the topography of the surface. The AFM can image nonconducting and conducting samples, because it uses an optical technique to sense the position of the tip relative to the sample.

One of the most common modes in which the AFM is used is the contact mode. The AFM is then operating in the repulsive region. The cantilever is bent away from the sample, since it is being repelled by repulsive forces. In this region the contact force, which is strongly dependent on the distance between the tip and the surface of the sample, is kept constant by a feedback loop (constant force mode). The size of the force has influence on the image which is made of the sample. For example, a scan has to be made with a force large enough to provide the image contrast, but at the other hand this will introduce deformation of the sample (or the tip, depending on which material is the softest). A force curve shows how the force is extended and retracted from the surface of the sample and the size of the contact force while scanning.

Using series of measured force curves taken over the same areas on a variety of samples a comparison between the different force curves is made. Additionally a relationship between changes in a force curve of an image and the vertical and lateral resolution of that image will be inferred.

Due to the twofold of the objective this report can generally be divided into two parts, though some of the information collected in the first part of this project is used the second part. The first part contains chapter 2 till chapter 4, chapter 5 and 6 together form the second part.

First in chapter 2 the interactions between the tip and the sample during measurements are analyzed. Then in chapter 3 the ideal shape and calibration of the force curve are discussed, just as the method to subtract the magnitude of the contact force from the force curve. In the last chapter of this part, chapter 4, the measurements of force curves on three different samples are analyzed. The last paragraph of this chapter

contains the general conclusions and recommendations which follow out of the comparison between the different force curves made on a variety of samples.

In chapter 5 the difficulties concerning image interpretation are described. Additionally in chapter 6 the measurements concerning the relationship between images and force curves are analyzed. The last paragraph of this chapter contains the general conclusions and recommendations concerning a relationship between images and force curves.

This report is based on measurements done with a Nanoscope II of Digital Instruments

1.2 The Nanoscope II

The Nanoscope II relies on three main parts: the optical head, the scanner and the base. Figure 1.1 shows a schematic picture of the optical head of the Nanoscope II , and figure 1.2 shows a front view of the complete Nanoscope II.
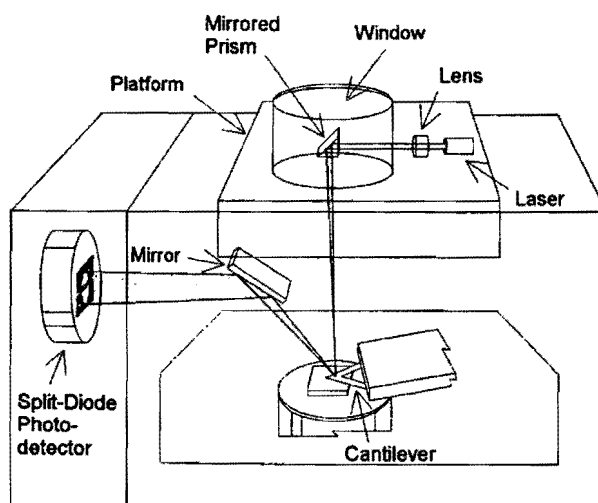
Figure 1. 1

The Nanoscope II has a very sharp tip which protrudes from the underside of a small, flexible cantilever. A laser beam, focused on the back of the cantilever, reflects off the top side of the cantilever onto a split photodiode. Height variations on the sample surface deflect the cantilever causing the position of the laser beam on the photodiode to change. The differential voltage from the photodiode elements provides a sensitive measure of the cantilever deflection (surface height of the sample).

The Nanoscope II scans the sample in a raster pattern while outputting the cantilever deflection-error signal to the control station. The digital signal processor (DSP) in the Workstation controls the Z-position of the piezo based on the cantilever-deflection error signal. The Nanoscope II operates in either a "constant height" or a "constant force" mode. The DSP always adjust the height of the sample under the tip based on the cantilever -deflection error signal, but if the feedback gains are low, the piezo remains at a nearly "constant height" and cantilever-deflection data is collected. With the gains high, the piezo height changes to keep the cantilever deflection nearly

5

constant (therefore, the force is constant) and the change in piezo displacement is collected by the system.
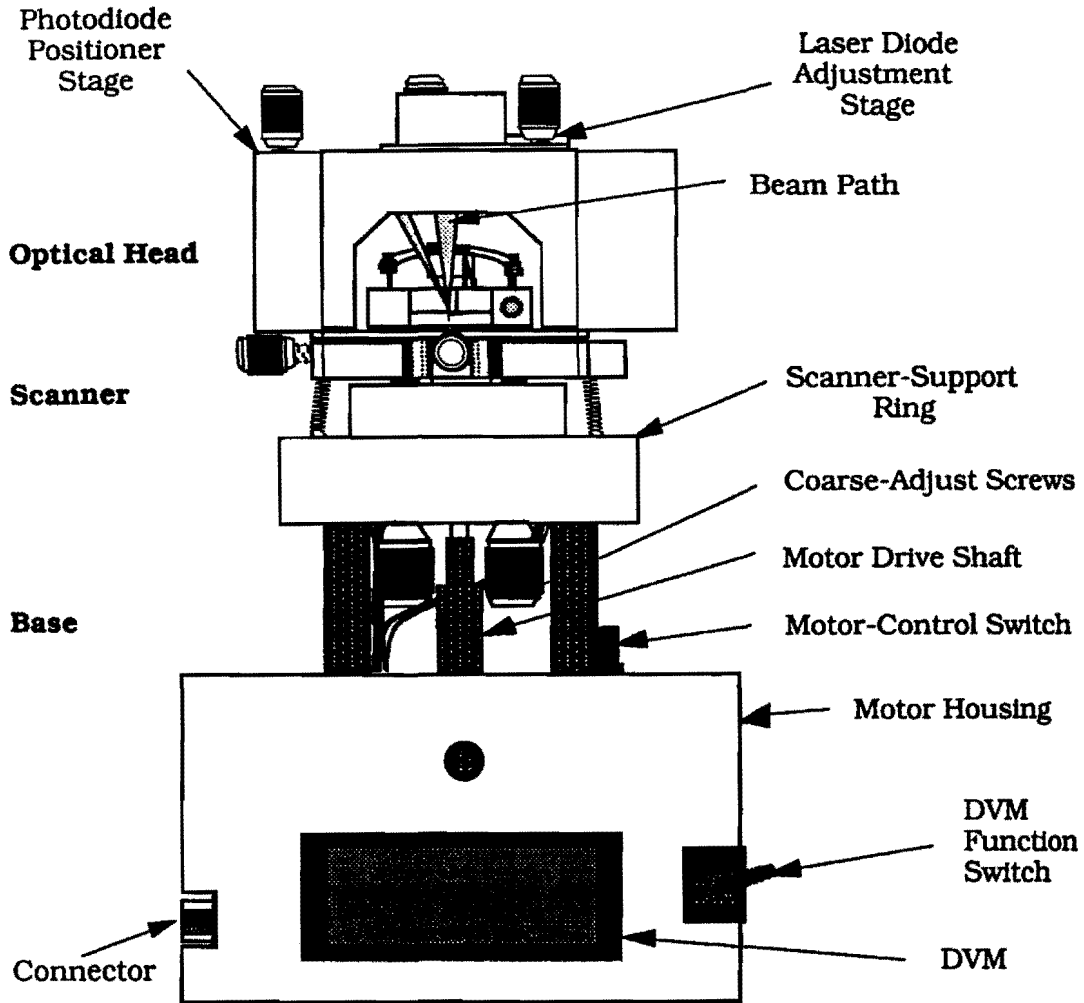
Figure 1. 2

Due to the weight of the optical head, the sensing system cannot be mounted on the piezo tube; therefore, the optical head and the probe are held stationary while the sample is scanned under them.

The scanner consists of a cylindrical piezoelectric tube which is rigidly held at one end with the sample mounted on the other end of the tube. The scanner also contains three fine-pitched screws which form the mount for the optical head. The optical head rests on the tip of the screws which are used to adjust the position of the head relative to the sample.

The scanner fits into the scanner-support ring mounted on the base of the microscope. Two of the screws on the scanner are operated manually while the third is controlled with a stepper-motor built into the base switch on the upper surface of the base and automatically by the computer during the tip-engage and tip-withdraw processes. The base also houses electronic circuits which are essential to the alignment and operation of the microscope. The LCD display of the digital voltmeter displays different signals depending on the position of the digital voltmeter Function switch.

Chapter 2

Interaction between tip and sample

The interaction between the tip and the sample takes place by interaction forces and sometimes deformation caused by the interaction forces.

2.1 The interaction forces

The interaction forces between the tip and the sample are:

- Van der Waals force. This force is caused by a fluctuation in the dipole moment of one atom (or molecule) inducing a dipole moment in another atom which are interacting with each other. The force can be either attractive or repulsive. The latter happens for the interaction of different bodies immersed in a medium, when the refractive index and dielectric constant of the medium have values lying between the corresponding values of the bodies. The force works on distances that extends from 2 Å to more than 1000 Å. The magnitude of this force is estimated to be in the 1-20 nN range [10].

- capillary force. This is an attractive force arising because of the surface tension of liquids. In atmospheric conditions there is usually a water layer on the sample that pulls the tip to the sample surface. This force can be strong and erratic because of strong dependence of surface energy and film thickness (ranging from 25 and 500 Å). Under ambient conditions this force is in the 10-100 nN range [14].

- repulsive force. This force is the result of the overlap potential between sample and tip atoms and change very strongly by change in distance. The magnitude can be as large as some tens of nN, and it takes place while the distance between the tip and the sample is less than 2Å [12].

- resonance force or exchange force. This force is causes by the resonance of the electron in the 1s state back and forth between two protons A and B. This force only takes place while the tip and the sample are both of conducting material and when the distance between tip and sample is between 2 and 8Å and is in the order of magnitude of nN [12].

- frictional force. This force opposes the motion of the tip relative to the sample. This force is related to the external force F_{ext} applied between two bodies by $\mu * F_{ext} = F_{fr}$. A recent study of Salmeron and co-workers [9] with a silicon nitride tip on mica showed that frictional forces are proportional to the normal forces in the moderate range (10-80 nN with a friction coefficient in the order of magnitude of 10^{-4}), in agreement with the friction behavior of macroscopic systems.

- adhesion. This is the general name for the intermolecular forces which tend to cause tip and sample to stick together. This can lead to a chemical bonding when the surfaces are brought together under compression. For this force values up to 100 nN are common in air [19].

- electrostatic force. This can be either a repulsive or an attractive force due to the build up of charge on tip and sample. This is rare since any excess charge will generally bleed to ground.
- magnetic force. This force might interact, dependent on the material properties of the tip and the sample.

2.2 Deformation

During operation to get atomic resolution, the contact area is theoretically just one atom. During operation for nanometer-resolution, the diameter of the tip-sample contact area is on the order of magnitude of nanometers. Because of this small contact area (in both situations) and a relative large scanning force, the pressure on the surface (force/contact area) of the sample is often too large and the sample (when it is the softest material) starts to deform. In addition the AFM provides atomic-scale images of the surfaces deformed by the tip force during scanning. Therefore, invaluable information about the nanomechanical surface properties can be obtained by these methods. How the sample surface is deformed under the tip force (when the tip is harder than the sample) can be tentatively envisioned as follows. The region of the sample in contact with the tip undergoes a macroscopic deformation as predicted by the continuum theories (for example the Hertz theory) in which the sample is regarded as a body of homogeneous density distribution. In most cases of chemical interest, the surface of a sample consists of atoms with several different environments, so that the local hardness of the surface varies from place to place. Therefore, the strong tip force induces a surface deformation according to the local hardness variation. Such a deformation, which can be on the nanometer or even atomic scale, is superposed on the macroscopic one, as shown in figure 2.1 [14].
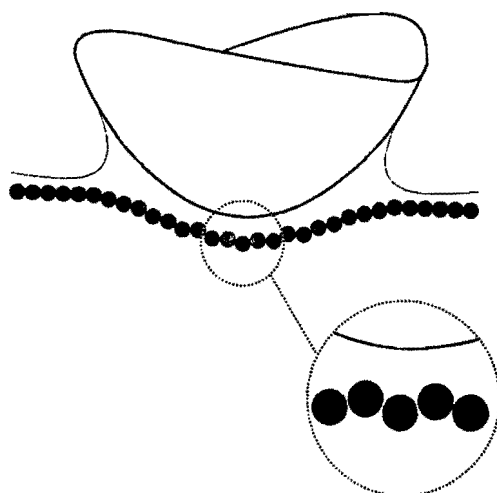
Figure 2. 1

Chapter 3

The force curve

3.1 The shape of the force curve

To check the interaction between the cantilever and the sample surface a force curve is used. While making a force curve the X and Y voltages applied to the piezo tube are held at zero and a sawtooth voltage as depicted in Figure 3.1 is applied to the Z electrodes of the piezo tube.
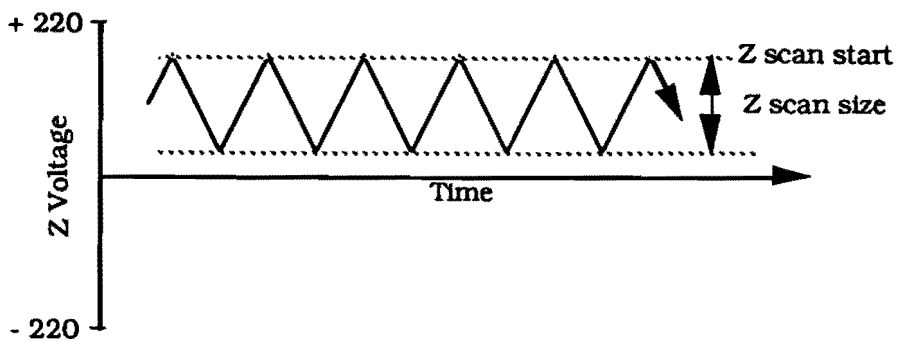
Figure 3. 1

As a result of the applied voltage, the sample is moved up and down relative to the stationary cantilever tip. The Z-scan start parameter sets the offset of the piezo travel while the Z scan size parameter defines the total travel distance of the piezo.
As the piezo moves the sample up and down, the cantilever-deflection signal, which is the difference in the voltages produced by the upper and lower photodiode elements in the optical head, from the photodiode is monitored.

Figure 3.2 depicts a typical force curve showing the desired features of the curve while Figure 3.3 shows the relative positions of the tip and the sample for the six points labeled on the curve.

Cantilever Off Surface

Cantilever Deflection Voltage

+Z
(Scan start)

Z Piezo Voltage

-Z
(Scan start -
Scan size)

Setpoint

Slope = Volts of Deflection/nanometers (or volts) of piezo travel

Figure 3. 2

Piezo travel
direction

Up   Up   At top   Down   Down   Down

Position   1   2   3   4   5   6
number

Figure 3. 3

The vertical axis of the graph represents the cantilever deflection signal. The voltage applied to the Z electrodes of the piezo tube is plotted along the horizontal axis. The left side of the graph is equal to the Z scan start, which is the maximum voltage that is applied to the Z electrodes of the piezo or the maximum distance covered by the piezo (depending on the units in which it is given) during the creating of a force curve. The right side of the screen is equal to the quantity Z scan start-Z scan si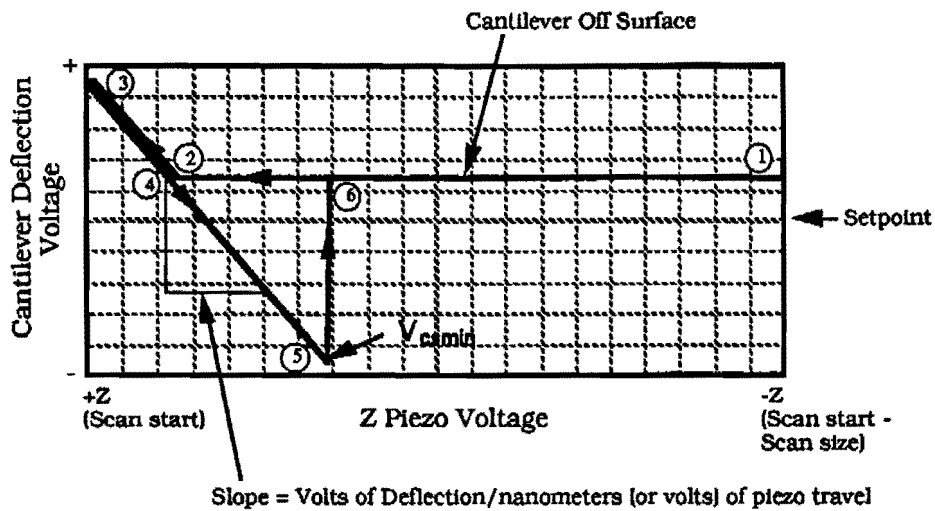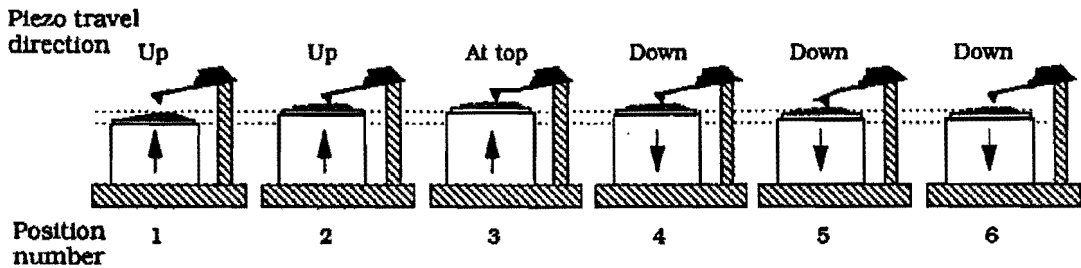ze, in which Z scan size defines the amplitude of the triangular wave form applied to the Z piezo, as shown in figure 3.1. The force curve represents the deflection signal for one complete extension/retraction cycle of the piezo.

At point 1 the tip is off the sample surface; the right side of the graph represents the most retracted point in the position of the piezo. From point 1 to point 2 there is no change in the deflection signal as the piezo extends, because the sample has not come into contact with the tip. At point 2, the sample contacts the tip and the deflection signal begins to increase. Often, there will be a slight dip in the deflection signal just as the tip reaches the sample surface, because attractive forces between the tip and the sample cause the tip to bend down to the sample surface. Then, the deflection signal continues to increase as the piezo moves the sample up. The deflection signal reaches a maximum at point 3, the maximum piezo extension; then, the piezo starts to retract. The deflection signal decreases as the piezo and sample retract. Typically, the signal continues to decrease after the flat, zero deflection point of the force curve, At point 4, the cantilever is not deflected, but due to attractive forces between the tip and the

sample, he tip sticks to the sample, and the cantilever is bent down as the piezo continues to retract. Eventually, the spring force of the bent cantilever overcomes the attractive forces, and the cantilever quickly returns to its non deflected, non contact position. This is represented by points 5 and 6 on the example curve. At point 5, the spring force of the cantilever equals the attractive forces between the tip and the sample. At point 6, the cantilever has returned to its undeflected state. Then, the cantilever deflection signal remains constant as the piezo continues tot retract to point 1.

For obtaining a force curve with the Nanoscope II the following parameters have to be set:

- Z scan start - This parameter defines the maximum voltage applied to the Z electrodes of the piezo during the force calibration operation, as shown in figure 3.1. The units of this item are Volts or nanometers, depending on the setting of the Units parameter.
- Z-scan size - As shown in figure 3.1, this parameter defines the amplitude of the triangular wave form applied to the Z piezo. the units of this item are Volts or nanometers, depending on the setting of the Units parameter. Regardless of the size of the scan, the entire scan is shown in the force curve.
- Graph range - This parameter defines the vertical scale of the cantilever deflection signal versus Z voltage graph.
- Setpoint - This parameter defines the centerline of the vertical, "Cantilever Deflection Voltage", axis of the force curve. Changing the setpoint shifts the force calibration curve on the graph.
- Sensitivity - This item relates the cantilever deflection signal to the Z travel of the piezo. It equals the slope of the deflection versus Z Voltage line when the tip is in contact with the sample. This parameter can be expressed in terms of the photodiode voltage versus the distance traveled by the piezo, or the voltage applied to the piezo, depending on the setting of the units parameter. The calibration of this parameter will be explained in the next paragraph about the calibration of the force curve.
- Units - To define the parameters on the horizontal axis this item select the units, either metric lengths or volts.
- Z scan rate - this parameter defines the frequency, in Hz, of the Z piezo oscillations during the force calibration procedure.
- Number of samples - This parameter defines the number of data points captured during each extend and retract operation of the Z piezo during the force calibration procedure.

3.2 The calibration of the force curve

Before accurate deflection data can be obtained the Sensitivity must be calibrated. The Sensitivity is equal to the slope of the force curve while the cantilever is in contact with the sample surface. To calculate the sensitivity the following steps have to be completed:

- Obtain a force curve on the display, which has a similar shape as the ideal force curve and which shows a contact force in the order of magnitude that can be expected according to the theory.
- Drag a best fitting line segment to the steeply-sloped portion of the curve.

Calculate the slope of the line segment and enter the calculated value as the sensitivity in the menu.

3.3 The contact force

The force curve clearly shows the relationship between the Setpoint and the deflection signal maintained by the feedback loop. If the spring-constant, k, of the cantilever is known, the force curve can be used to calculate the contact force of the tip on the sample. the contact force is defined by the equation:

$$F = k\Delta z$$

where Δz is the z distance from the control point to the pull-off point in nanometers. Figure 3.4 shows an imaginary force curve;

Z Position - 10.0 V/div
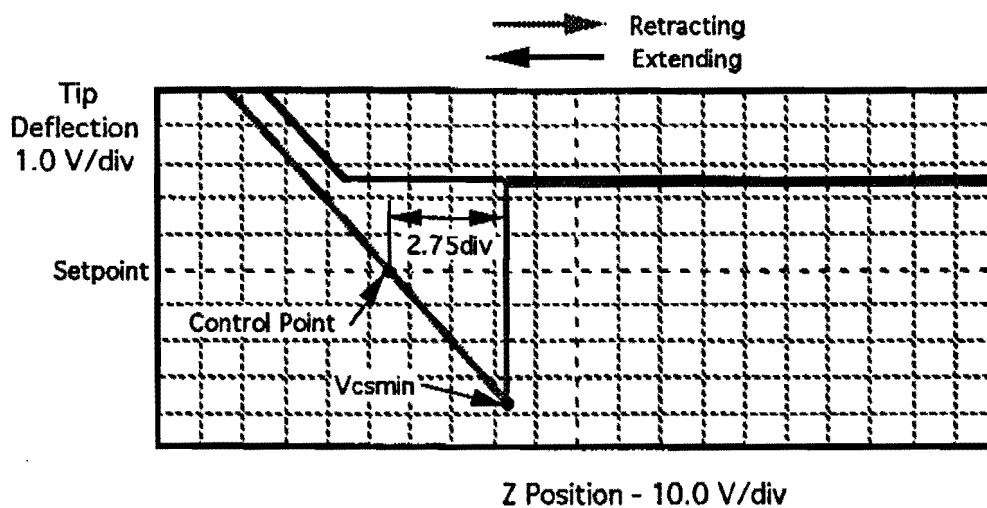
Figure 3. 4

The calculation of the contact force is as follows:

$$F = k\Delta z$$
where:
k = 0.6 N/m
Z piezo sensitivity = 2 nm/V
Δz = 2.75 div * 10.0 V/div * 2 nm/V = 55 nm

F = 0.6 N/m * 55 nm
 = 33 nN

12

Chapter 4

Measuring force curves

4.1 Experiments and Results

Force curves were made on several different samples, chosen from the available samples in the lab. The samples were of mica (muscovite), graphite(Highly Ordered Pyrolytic Graphite (HOPG)) and gold. Before using the graphite sample it was cleaned by pressing some sticky tape to the surface and pulling off a layer of material. On the mica and gold sample, force curves were made before and after cleaning the samples with methanol. With the cleaning of the samples, the waterlayer, which covers the surface of the sample in ambient conditions, is removed. Six or seven measurements on a sample were made. Between these measurements the tip is only withdrawn and immediately engaged again (on a scan rate of 31.25 Hz). After five good engagements (which takes about 10 minutes) the sample is cleaned again. The force curves are made while looking at images of 10×10 nm, which made it impossible to see whether the new engagement was on the same spot as the last one or not. (For explanation see appendix A.)

In figure 4.1 the typical shape of a measured force curve is shown.
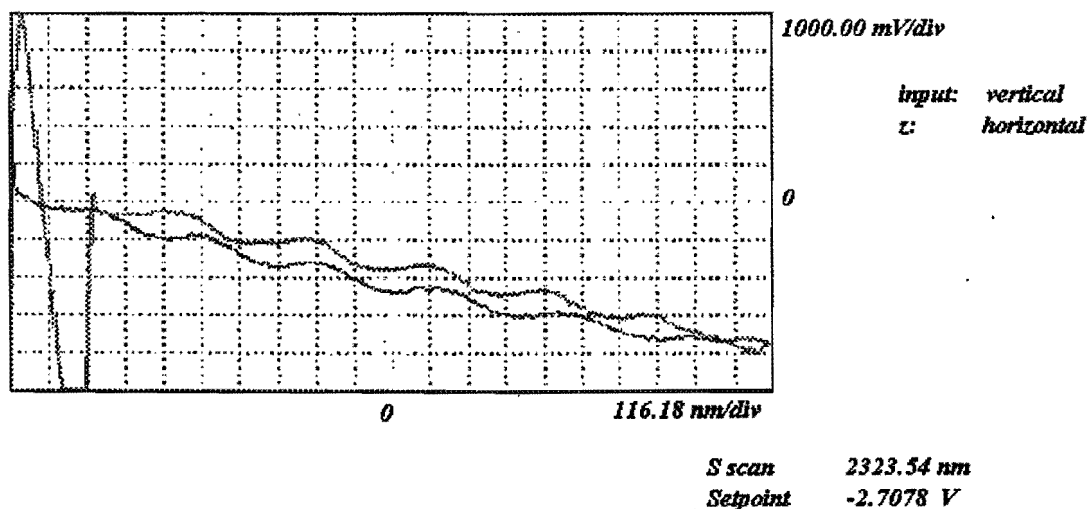

Figure 4. 1

The analyzing of this shape will be discussed in paragraph 4.2

In table 4.1 the magnitudes of the measured contact forces for the different samples are listed.

13

sample	Faverage [10^{-8} N]	Fmin [10^{-8} N]	Fmax [10^{-8} N]	range absolute [10^{-8} N]
mica	4.1	3.7	4.2	0.5
mica cleaned	1.6	1.4	1.9	0.5
graphite	1.0	0.7	1.1	0.4
gold	0.7	0.6	0.8	0.2
gold cleaned	1.2	0.8	1.5	0.7

Table 4. 1

The analysis of these forces will be discussed in paragraph 4.3.

4.2 Shape force curve

When we compare the shape of the force curves of our measurements with the shape of the ideal force curve we see two remarkable differences. While extending the tip to the sample the curves showed a positive slope and while retracting the tip from the sample the curves showed a negative slope, instead of a horizontal line in both situations. This line also shows a waving.

When the signal received by the photodiode is optimized it means that the (A+B)-signal is maximized and the (A-B)/(A+B)-signal is made 0. Two examples of optimized laserbeams are given in figure 4.2.

Figure 4. 2

Theoretically it is possible to influence the place of the beam in the horizontal direction. This horizontal deviation depends on the possible torsion of the tip and the angle made by the mirror in the horizontal direction. This last angle can be influenced, but because it only has to change a really small angle and the mirror can only be aligned roughly it is practically impossible to place the laserbeam exactly in the middle of the diode.

To engage the tip on the sample the (A-B)/(A+B)-signal is made negative, so that after engagement the signal is in the middle of the photodiode. This is shown in figure 4.3.
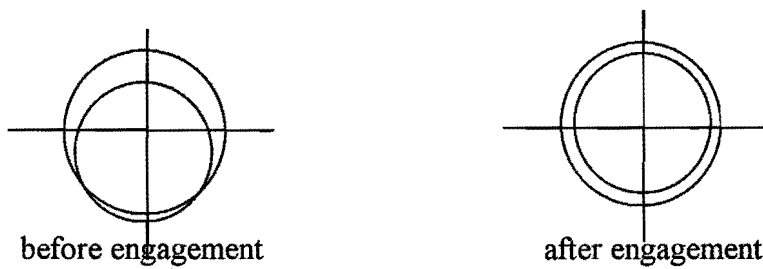
before engagement   after engagement

Figure 4. 3

Often this is not the case, the beam is still under the middle. This can be seen in the force curve, where the horizontal line on which doesn't have any deflection starts on a (A-B)/(A+B)-signal less than 0.

The intensity of the laserbeam has a gaussian distribution. The center of this beam is reflected on the cantilever. The rest of the beam is reflected from the sample. Because the center of the beam will be reflected on the cantilever, there will be much more light reflected from the cantilever than from the sample. The reflected beams both are assumed to be gaussian. Though the intensity of the beam reflected from the sample will be much lower than the intensity of the beam reflected on the cantilever. The two reflected lightbeams will interfere with each other which causes an interference pattern on the photodiode. This interference pattern will be an alternation of maxima and minima, as showed in figure 4.4. In which the dashed lines are maxima and the dotted lines are minima.
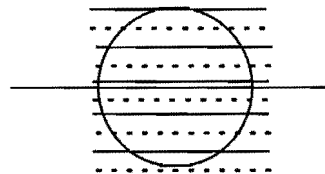
Figure 4. 4

According to the interference theory of light [8] the distance between two alternative maxima, Δy, can be calculated by

$$\Delta y = \frac{\lambda}{2}$$

In which λ stands for the wavelength of laserlight ($670*10^{-9}$ m). Looking back in figure 4.1 it is seen that the distance between two maxima in the waving is 3 divisions. Every division represents 116.18 nm in horizontal direction, so the distance between two maxima is 348.5 nm. Using the relation above a wavelength of 697 nm is found. This shows that the waving in the force curve is caused by the interference of the laserlight reflecting from cantilever and sample.

4.3 Contact forces

In this paragraph the attention is focused on two matters, the accuracy and the magnitude of the measured forces.

4.3.1 accuracy contact forces

In paragraph 3.3 is already shown how the contact force is calculated by using the force curve, $F = k*\Delta z$. This means that the accuracy of the force is dependent on the accuracy of k and Δz.

Accuracy can be expressed by looking at the relative error of the measurements. This error is defined as $\dfrac{\Delta a}{a}$, where Δa and a are respectively the maximum absolute error and the assumed value.

Distance Δz can be measured properly to 0.2 divisions of the horizontal axis of the force curve. During measurements the scale is adjusted to the seize of the force which is measured in that way that Δz always covers at least 1 division. So the relative error, in the worst case, is 0.2.

The accuracy of springconstant k is determent by the requirements of the cantilever, which are given in the productcatalogue of Park Scientific Instruments. This says;

    k = 0.32 N/m when the thickness of the cantilever is 0.6μm. Though the cantilever thickness can actually vary from 0.4μm to 0.7μm.

To calculate the change in stiffness the equation for the cantilever stiffness in normal direction presented by J.M. Neumeister and W.A. Ducker [16] is used. This equation shows that thickness is cubed in the springconstant calculation. This makes that the springconstant is ranging from 0.09 N/m (for t=0.4μm) to 0.51 N/m (for t=0.7μm). For all the force calculations in this report k=0.32 N/m is used. This gives a maximum relative error of 0.7.

The accuracy of the contact force is calculated by,
$$F = \Delta z * k$$
$$\delta F = \delta(\Delta z)*k + \delta k*(\Delta z)$$
$$\delta F/F = \delta(\Delta z)/(\Delta z)+\delta k/k = 0.2+0.7 = 0.9$$
This extreme large relative error is mostly due to the changes in stiffness between the different tips.

This error can be reduced a lot if the springconstant of the used cantilever is determined with an nondestructive method. One method is described by Torii et al [18], by using a calibrated large-scale cantilever and measuring the deflections of both cantilevers simultaneously using heterodyne interferometry. Another method is described by Smith and Howard [17], by using a novel precision force balance measuring the distortion of the cantilever while varying the added force. A third non destructive method is described by Cleveland et al [6], by measuring the resonant frequencies of the cantilevers before and after adding small end masses. They did measurements on four 120-μm-long, 22-μm-wide V-shaped silicon nitride cantilevers (supplied by Digital Instruments, Santa Barbara), three from different locations in a single wafer and one from a second wafer. The three had similar measured spring constants, 0.10±0.01 N/m, while the fourth had a measured spring constant of 0.36 N/m. Carefully, we can conclude that the tips from one wafer have almost the same stiffness. During the experiments executed for this report the used cantilevers were all

taken from the same wafers so the stiffness of the tip will not change a lot from tip to tip. This makes it allowable compare the forces measured on different samples to each other.

But due to the "unknown" stiffness of the cantilever for a quantitative analysis only the order of magnitudes of the measured forces can lead to conclusions.

4.3.2 order of magnitude contact forces

The measured curves showed forces of the magnitude 10^{-8} N, for the mica and graphite samples. With the interaction forces mentioned in paragraph 2.1 in mind we can conclude that this is just as expected. Though for these samples there is also another reason why the forces measured are bigger than the order of magnitude of 10^{-9} N, which are forces on atomic scale. The explanation is found in the structure of the material. These materials have a layered structure. During scanning the tip is in mechanical contact with the surface of the sample. There is a repulsive force between the tip and the sample, this force generates a compression of the surface of the sample.(For graphite this compression can be as large as a few angstroms) because of this compression, the change in gap width is much smaller than the observed z displacement of the Z piezo. so, the Z piezo has to displace more than without compression. Because the contact force is calculated as $\Delta z*k$ this force appears greater than it actually is. Because of this effect, forces as large as a few hundreds of nN can be measured. So the measured force curves of graphite and mica are as could be expected.

The difference between the forces measured on the cleaned and the uncleaned mica sample is because the cleaning removed the eventual contamination layer and/or the capillary force. After the cleaning even the range of the measured forces is reduced, this can be due to the fact that the waterlayer which causes the capillary force is not very homogeneous. The effect of the layered material is more homogeneous.

The magnitude of the force measured on the gold sample is also in the order of 10^{-8} N. For this large force there are two different explanations. First it could be due to an existence of a contamination layer. But at the other hand it also could be because of a big difference between the dielectric constant and the refractive index of the gold and the tip material which is Si_3N_4. According to Lifshitz theory (13), the Van der Waals forces are considered as dispersion forces associated with the electromagnetic fluctuations. This theory shows that the forces between bodies interacting through a medium depend on the dielectric properties of the bodies and the medium. The larger the difference the larger the van der Waals force. The larger the van der Waals force, the bigger the snap of the tip in the material. The tip will snap into the surface of the sample from a larger distance and with a bigger force. The surface of the sample will deform more. The dielectric constant of Si_3N_4 is 6.34 and the refractive index is 1.986. For gold the refractive index is between 0.24 and 1.86, unfortunately I still haven't been able to find out the dielectric constant.

After cleaning the gold sample, the force curves showed a contact force twice as big as before cleaning the sample. Both explanations mentioned above can be combined to explain this difference. It could be possible that this is because of the removing of the contamination layer, and a bigger difference between the constants just mentioned

17

between the tip material and the gold than between the tip material and the contamination layer.

The large range of the measurements of the forces on the gold sample can be explained as follows. When we look on the gold sample using a microscope we see all kinds off scratches, they can be responsible for a strong inhomogeniety of the surface of the gold sample. A scratch is due to a plastic deformation of the gold in an area which is much larger than the scratch itself. Because there are so many scratches it is not possible to make an image on an area which is not close to a scratch. Plastic deforming causes a different local hardness of the material. The hardness of the material is one of the parameters which influences the magnitude of the contact force. The contamination layer can cover this differences in hardness. This can be the reason that the large range of the measurements of the forces does not exist in the measurements of the uncleaned sample.

From these observations it can be concluded that while investigating the relation between the force curve and the image of a sample, the structure of the material and the difference between the dielectric constant and the refractive index of the tip and the sample should be taken into account.

4.4 Repeatability of measurements

In general the repeatability of the force curves is limited because of three reasons:
- The condition of the tip is important for the repeatability of the measurements. During a series of measurements the condition of the tip is changing. Before getting a force curve, the tip always vibrates, which attacks the good condition of the tip. This is due to the fact that the control unit of the AFM, when changing to the Force mode, automatically start with a large z-scan-size and z-scan start value, often much larger than necessary, to show a force curve. The only thing that can be done by the user to reduce this vibration, is reducing these values to small values as quick as possible. From that (new) start situation the parameters are raised slowly.
- Deformation of the surface due to the contact force, has impact on the surface quality. The surface quality is of influence on the measured force. On some samples it is obvious that there will be deformation. On graphite for example, forces in the order of magnitude of 10^{-8} N were measured. The tip radius, of the tips used for these measurements, is between 20 and 60 nm. This means that there is a contact area with a radius of several nanometers. If a contact radius of 20 nm is assumed, then there is a contact area of $1.3*10^{-17}$ m^2. This leads to a pressure on the sample of $10^{-8}/1.3*10^{-17} = 7.7*10^8$ Pa. Comparing this pressure with the compressive strength of graphite, $5.7*10^7$ Pa shows that there will be deformation.
- The re-engaging on the same place on the surface is important for the repeatability of a force curve. The magnitude of the force is very dependent on the surface which is measured. Small changes in the surface quality cause already a significant change in the force. This is made clear with the following experiment, in which all the force curves are made on different crystals of diamond. The measured forces are listed in table 4.2.

curve nr.	F $[10^{-8}\ N]$
1	2.1
2	37.8
3	37.5
4	9.0
5	32.7

Table 4. 2

This results show is that, though the force measured on crystal 2 and 3 is almost equal, there is a big spread between the forces measured on the crystals.

4.4.1 AFM-re-engagement repeatability

It is shown that force curves made on different crystals differ a lot. So for investigating the repeatability of force curves we need to be sure that we are making the force curves on the same place on the sample. Therefore before investigating the force curve repeatability is investigated first the re-engagement repeatability of the nanoscope II is investigated.

The AFM does not re-engage on the same spot on the surface. In order to get information about the accuracy of re-engagement an experiment using a sample of a 0.3 μm diamondfilm grown on (100) silicon was done. When different images of graphite or mica on atomic scale are made we cannot notice features on atomic-scale (see appendix A page 36). Larger features are most of the time so big that they disturb the whole image. On a sample like graphite it is difficult to detect whether we are on the same spot or not.

A sample of diamond on silicon gives a clear image on a scan size of 4000 nm with features which are easy to recognize. The mica, graphite and gold give only clear pictures with a much smaller scan size on which it hardly can be seen if the engagement is on the same spot or not.

On the diamond sample several images where made between which the tip is only withdrawn and re-engaged without changing anything else. The place of withdrawing was chosen random, and the scan rate was all the time 31.25 Hz. The results are included in Appendix B on page 37. Taking the lower left corner of the image as a reference point, the distance from that point in x and y direction to a certain crystal was measured. The differences between the measured value for x and y for two alternative taken images is called Δx and Δy:

$$\Delta x_{average} = 203\ nm \qquad \Delta x_{max} = 271\ nm \qquad \Delta x_{min} = 68\ nm$$
$$\Delta y_{average} = 834\ nm \qquad \Delta y_{max} = 1153\ nm \qquad \Delta y_{min} = 272\ nm$$

This large differences in y-direction could have been caused by a few different reasons:

• The different places of withdrawing. Perhaps the tip will have a different x and y offset at different places..

• Vibration of the cantilever. While withdrawing at a high scan rate the cantilever vibrates in the x and y direction because the friction force is suddenly reduced to zero. After this vibration the cantilever may have a little plastic deformation left.

19

• The deflection of the cantilever before engagement. Before engagement the cantilever has a certain deflection which corresponds with a certain voltage of the (A-B)/(A+B) signal. After making an image and withdrawing, the voltage often differs from the voltage before making the image, this means that the deflection of the cantilever is not the same as before imaging. This happens because the cantilever is withdrawn with steps in distance between 1 and 2 μm. The force, and thus the cantilever deflection, has a strong relation with the distance, so an extra withdraw step can change the deflection of the cantilever more than necessary to get the deflection from before imaging. This is shown by the (A-B)/(A+B) signal, this signal should be the same before engagement and after withdrawing.

To check the influences a few experiments were done. During the first series of measurements the voltage of (A-B)/(A+B) before engagement was always the same. The scan rate before withdrawing the tip was reduced to 4.34 Hz. The tip was always withdrawn at the bottom of the image. This restriction improved the accuracy of engagement in y-direction. Also was noticed that if the voltagesignal (A-B)/(A+B) after withdrawing is close to the one before engaging the next engagement is much closer to the last one than when this voltages change a lot. When the voltage becomes positive after withdrawing the accuracy of the next engagement is even worse comparing to the same amount of change in voltage but in the negative direction. The results of this experiment are shown in table 4.3.

During the second series of measurements, the withdrawing of the tip was again always at the bottom of the image. But now we reduced the scan rate before withdrawing to 0.18 Hz. The results of this experiment showed a good repeatability again. This time it was again noticed that the value of the (A-B)/(A+B) voltage, which shows the deflection of the cantilever, is important. For the best results the voltage before and after have only a spread of +/- 0.1 Volt. These results are also showed in table 4.3. During the last experiment the same restriction as in the second experiment were followed, only the place of withdrawing the tip was chosen random. Table 4.3 shows al the results:

exp.nr.	$\Delta x_{average}$ [nm]	Δx_{max} [nm]	Δx_{min} [nm]	$\Delta y_{average}$ [nm]	Δy_{max} [nm]	Δy_{min} [nm]
1	203	271	136	380	1085	0
2	23	34	0	57	102	0
3	135	203	68	113	203	34

Table 4. 3

Because the results of experiment 3 are worse than the results of experiment 2 it seems that the place of withdrawing is of influence. But the voltages after withdrawing during the second experiment were much more equal to the voltages before engaging than during the third experiment. The worse results are due to this difference.

What also is important in interpreting the results is the facts that the way of measuring the differences of engagement had an accuracy of +/- 40 nm. So the accuracy is small compared to the measured values. The accuracy is that bad, because of two reasons. The first is that with the mouse a large cross is clicked in the points between which we want to know the distances. Because the cross is that large it is difficult to see if exact the same place as before is clicked. The other reason is that the resolution of the

images (4000*4000 nm) on which the distances are measured is not so good that it is clear if the same place on the crystal is touched.

To get the best repeatability of engagements two things are important:
1. The (A-B)/(A+B) voltage after withdrawing from image 1 has to be the same (within a spread of +/- 0.1 V) as before the engagement for image 1, to get a good re-engagement for image 2.
2. Before withdrawing the scan rate has to be reduced (till around 0.2 Hz)

To check these conclusions a control experiment was executed. The results are listed in table 4.4. In this table the voltage corresponds with the voltage after withdrawing from the tip and which is at the same time the voltage before the engagement for the next image. The Δx and Δy corresponds with the difference in place of engagement in the x- respectively the y-direction comparing to the engagement before.

engage- ment nr.	voltage [V]	Δx [nm]	Δy [nm]
1	-2.13	-	-
2	-2.27	20	320
3	-2.30	0	70
4	-2.36	20	40
5	-2.35	10	10
6	-2.39	0	0

Table 4. 4

In one view it is seen that the voltage between the first and second engagement differ remarkably more than between the other engagements. This shows also up in the Δy value at the second engagement. Removing this measurement gives us the next results:

$$\Delta x = 7.5 \text{ nm} \qquad \Delta y = 30 \text{ nm}$$

The range in which we can repeat the engagements makes it possible to look, with the use of the x and y offset, at the same image after several engagements.

4.4.2 Force curve repeatability

To determine the repeatability for force curves made on the same diamond crystal 5 force curves were made by imaging the same crystal at a 100*100 nm scan size. It is sure that the force curve is made on the same crystal, but not if it is made on exactly the place on the crystal.
The measured forces are listed in table 4.5:

eng. nr.	F [10^{-8} N]
1	4.8
2	12.5
3	12.4
4	11.3
5	9.7

Table 4. 5

$$F_{\text{average 2-5}} = 11.5*10^{-8} \text{ N} \qquad \text{range } F_{2-5} = 2.8*10^{-8} \text{ N}$$

At first it is noticed that the first measured force is remarkably lower than the others. this can be due to the cleaning with methanol. A drop of methanol is put on the sample. After a few seconds the methanol is removed with a laboratory wiper by just putting it on the sample and removing it again. The methanol which is left after that will evaporate quickly. After this process, the sample is a little colder than it's environment so a small waterlayer is formed quickly again. When the first measurement was made the sample didn't have the waterlayer already, or it was only starting to form itself. When the rest of the measurements are taken the waterlayer was already on the sample. The magnitudes of the forces agree with this explanation. The capillary force has a magnitude estimated between 10 and 100 nN (see paragraph 2.1). The difference between the first and the average of the four other measurements is $6.7*10^{-8}$ N.

The range of the forces is acceptable because we are measuring in air and without a cover for the AFM, so the measuring conditions are not very constant.

4.5 Conclusions and Recommendations

All the information presented in this chapter leads to a few general conclusions and recommendations.

- The shape of the force curves measured with the Nanoscope II used for this report is different from the shape of the ideal force curve. The measured force curve shows a slope and a waving in the part of the curve representing the extending and retracting movement of the tip to or from the sample. (§4.2)
- While interpreting the results of the experiments, only the order of magnitude of the contact forces can be discussed. This is because the stiffness of the used cantilever is not known precise enough, it is only known that it is between 0.09 N/m and 0.51 N/m. The results will have a lot more impact when the stiffness is known much more accurate. In paragraph 4.3.1 three ways to determine the stiffness of the cantilever are presented. Unfortunately, the time for executing measurements according to one of these methods was not available.(§4.3.1)
- Though only the order of magnitude can be discussed, it is clear that the interaction forces (10^{-8}), while measuring with an AFM in ambient conditions, are much larger than atomic forces (10^{-11}). Using an AFM under ambient conditions, one really needs to be aware of these measuring forces. This is because they introduce deformation, make images showing hardness representations of the examined material instead of structure and so on. The forces can be reduced by

measuring under ultra high vacuum (taking away the capillary force) or under liquid (reducing the Van der Waals force and taking away the capillary force).(§4.3.2)

- For the repeatability of force curves it is important to re-engage on the same spot on the sample. The get the best results two things are important:
  1. The (A-B)/A+B)-voltage after withdrawing from image 1 has to be the same (within a spread of ±0.1V) as before engagement for image 1, to get a good re-engagement for image 2.
  2. Before withdrawing the scan rate has to be reduced (till around 0.2 Hz) (§4.4.1)
- For the repeatability of the force curves it is also important to have the same environmental conditions. The measurements used in this chapter are all done without a cover for the AFM. For sure the range would be less when the measurements were executed with a cover, therefore it would be useful to look for a cover for the AFM, to reduce distortions by noise, air movements and so on. Unfortunately the cover was available after finishing all the measurements for this part of the report. Time was not available to repeat measurements to have an indication of the impact on the measurements of the cover.

Chapter 5

Image interpretation

5.1 The vertical resolution

The vertical resolution of the AFM is depending on the system which is used to measure the cantilever deflection. As mentioned in paragraph 1.1, the Nanoscope II is using the optical deflection method. The theoretical sensitivity of the microscope can be calculated using Gaussian beam optics (as already explained in paragraph 4.2) and assuming shot noise. The minimum detectable cantilever displacement,) z, is given by [15]:

$$\Delta z = \frac{2}{3} * \left(\frac{S}{N}\right) * \left(\frac{1}{V\sqrt{2\pi}}\right) * \lambda * \sqrt{\frac{\Delta fe}{\eta P}}$$

where (S/N) is the signal-to-noise ratio, λ is the laser wavelength, Δf is the detection bandwidth, e is the electric charge, η is the spectral responsivity, P is the total power incident on the photodiode, and V (= $2\omega_0$/l) is the ratio between the Gaussian beam diameter $2\omega_0$ and the cantilever length l. The prefactor 2/3 comes from the fact that the cantilever is not rigid: its slope at the free end is given by $(3/2)(\Delta z/l)$. In the above equation, we assume that the photodiode is located in the far-field region of the beam, an assumption which is borne out in practice. Realistic values for the parameters, while using the Nanoscope II are, S/N= 10, λ= 670 nm, η= 0.4, Δf= 1 kHz, P=1 mW and V=1, this gives) z≈ 0.01 nm.

So the vertical resolution of the Nanoscope II is in the sub angstrom range.

5.2 The lateral resolution

The lateral resolution of the AFM is determined by two factors, the stepsize of the image and the tip-sample contact area.

Concerning the first factor, the stepsize of the image, figure 5.1 shows the scanning motion during data acquisition.
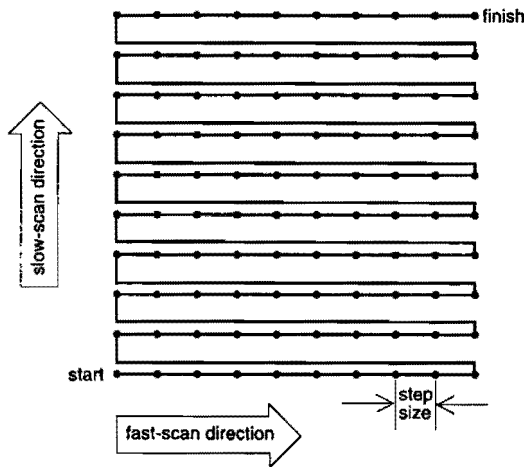
Figure 5. 1

The images, used for this report, are made with a sample size of 400, what means that in the fast-scan direction every line has 400 sample points and in the slow-scan direction the scan size is divided in 400 lines. It is clear that the scan size has an influence on the resolution. The maximum scan size which is used for the experiments is 4000 nm. this scan size gives a resolution of 4000/400 = 10 nm.

The resolution determined the tip-sample contact area is more complex to distinguish. The quoted *best resolution*, however depends upon how resolution is defined.

In microscopy community, two asperities (peaks) are considered resolved if the image satisfies Rayleigh's criterion [1]. This criterion requires that the height of the image dip is at least 19% between the asperities as illustrated in figure 5.2.
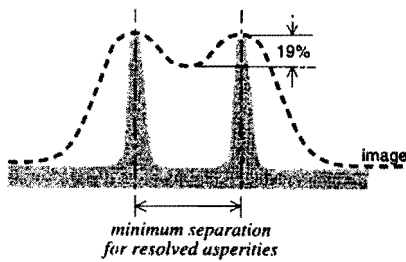

Figure 5. 2

The minimum separation between resolved asperities determines the best lateral resolution of the system.

Theoretically the lateral resolution with this criterion can be calculated easily.
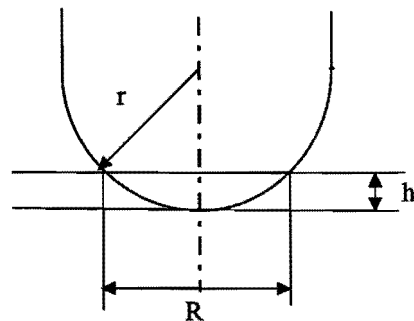
The shape of the used tip is as in figure 5.3

Figure 5. 3

In which r stands for the tipradius, h stands for the height of the image dip and R is the distance which is necessary between the asperities to be able to have an image dip of 19%, so is actually the resolution corresponding with a certain image dip.

For the resolution it is easy to derive, with the use of pythagoras, a relation which shows the dependence on the tip radius and the image dip.

25

$$R = 2 * \sqrt{r^2 - (r - h)^2}$$

In the experiments tips with a radius between 20 and 60 nm are used.

To give an idea of the size of the lateral resolution determined by the tip in table 5.1 for the two extreme tip radii and several different z-ranges, the lateral resolution is calculated in nanometers.

z-range [nm]	$R_{r=20}$ [nm]	$R_{r=60}$ [nm]
1	6.2	10.9
10	17.3	33.2
20	40	44.7
60	40 (=max.)	120

Table 5. 1

When the asperities which are measured are as long as or longer than the tipradius, the maximum resolution is reached. For a tipradius of 20 nm that will be 40 nm and for a tipradius of 60 nm that will be 120 nm.

In practice, contact-mode AFM operation with forces in the order of magnitude of hundred nanonewton, leads to well-resolved atomic-scale images for many inorganic layered materials. This finding is explained by the effective sharpening of the tip. The surface of the tip is not completely smooth. The shape of the tip will be similar to the shape in figure 5.4
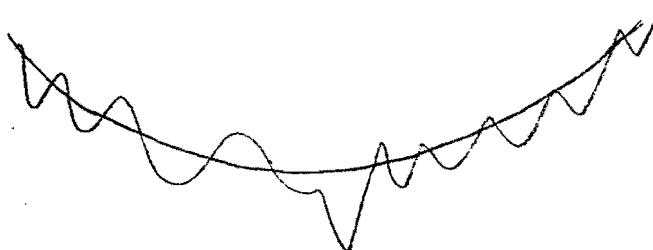

Figure 5. 4

The most protruding irregularity is used for scanning the surface. Still under a high applied force, the tip-surface contact area would be relatively large, but not all atoms of the tip in the contact area contribute equally to the total repulsive force between the tip and the sample. Since the repulsive force curve is very steep for small atom-atom distances, the total repulsive force may be dominated by the contributions of the few outermost atoms of the tip apex. This sharpening effect might lead to the detection of atomic-size defects.

This will only work on smooth surfaces, on rough surfaces the tip radius will be the determining factor for the minimum resolution.

5.3   Imaging

While imaging, it is important to understand that the operating force should be minimized to obtain reliable and high-resolution images and avoid an irreversible surface damage. In contrast it is also shown that the employment of strong applied forces (of the magnitude of hundreds of nN) are necessary to enhance the image

contrast. The induced surface deformation contributes strongly to the image contrast. This makes it possible to detect the presence of the different structural building blocks comprising their surface [4].

While imaging, it is also important to minimize the effect of the thermal drift on the geometrical parameters of the images. it is necessary to carry out imaging after thermal equilibrium has been reached between the sample and microscope stage, and to conduct measurement with a high scanning speed.

Images should be collected in the "up" and "down" scanning directions and at different rotation angles of the fast-scanning direction. Finally, the geometrical parameters of these measurements should be averaged. This procedure gives rise to more reliable surface parameters from the images.

5.3.1 large scale imaging

The interpretation of large-scale AFM images can be complicated when chemically or structurally different domains are present on the surface, because they might modify the local hardness and friction of the surface. This leads to more complicated image patterns than those expected from the surface topography. To confirm the surface-hardness contribution to the images, it is necessary to conduct force-dependent measurements by varying the set-point force level, since the image contrast between the hard and soft regions of the surface increases with increasing load. The softer region of a surface is expected to be more depressed by the tip force, which increases the tip-sample area.

In principle, it should be possible to distinguish different surface domains by utilizing the response of the AFM probe to the hardness, friction and different surface forces of a sample surface. In most cases, however, interpretation of the associated image contrast is not straightforward, because the surface hardness and friction are affected both by chemical structures and by their packing arrangements. To deconvolute the different factors contributing to the images, it would be useful to employ various chemically modified tips to emphasize, and thus identify, specific types of tip-sample interactions.

Another problem is often observed for a hard surface with steep corrugations. if a sample surface has structural features sharper than the tip apex, the imaging roles of the tip and the surface are reversed so that the tip shape appears in the image. The AFM is definitely limited in studying those surfaces.

For flat surfaces, with large scale and atomic scale imaging , image imperfections might occur due to a multiple tip effect. The image features associated with double-tip imaging are characterized by "ghost" patterns, in which the surface features are repeated.

Many image artifacts are not self-evident, so one should carry out repeated measurements to characterize properly the sample under examination. For large-scale measurements of corrugated surfaces, sharp tips are desirable; it is therefore useful tot test the tip shape with standard samples of known profiles. However this does not totally eliminate image artifacts, because a selected tip can be modified during scanning. Therefore, in the absence of reliable control of the tip apex geometry, it is common to employ several different tips for examination of a given surface and to

choose the most reproducible images as the genuine representations of the sample under consideration.

5.3.2 Atomic scale imaging

For atomic-scale patterns it is common to observe variations of the image details on the experimental conditions. Image variation may occur spontaneously due to the instability of the tip and the surface, even when the scanning is carried out without changing the experimental conditions. Alternatively, image variation may reflect a change in the tip-sample distance and applied force, so it can help to characterize the sample surface.

To understand the dependence of the image features on the applied force, it is necessary to carry out force-dependent measurements. For example, results of force dependent AFM experiments for layered telluride $NbGe_{3/7}Te_2$ shows for a low-force AFM a hexagonal pattern which is to be expected from the atomic arrangement of the Te-atom surface layer (14). In a high-force image however, periodic rows of depressed surface atoms appear; upon reducing the applied force, this feature disappears. These reversible image changes show the occurrence of reversible, atomic-scale surface relaxation. The high-force image reveals the variation of the surface local hardness. This will be discussed further in Chapter 6, for a graphite, mica, silicon and diamond sample.

Chapter 6

Measuring and analyzing images and their relationship with contact forces

6.1 Description of experiments

To look at the relationship between the resolution of an image and the used contact force, two experiments were done:

- During the first experiment the tip is engaged once and imaged for a long time, about an hour, the same place. Every ten minutes a force curve was made and an image was captured. Of course the force curve was made on a flat part of the sample. The force with which this imaging was done is the force just after engagement, which is depending on the snap into contact. After the force is set for the first measurement of the experiment in the middle of the graph nothing is changed during the rest of the experiment.

- during the second experiment the tip is engaged once and different images were made by different values of the contact force.
  The contact force can be influenced by changing the setpoint. The contact force is defined by $F=k\Delta z$, in which Δz is the distance between the control point and the pull-off point as mentioned in paragraph 3.3. By lowering the setpoint the control point is moved closer to the pull-off point, so the contact force is decreasing. The opposite happens when increasing the setpoint.
  The maximum change of the contact force is limited because the setpoint of the used AFM can only be changed from -10 to 10 V. An other obvious limitation is that the setpoint can only be lowered as long as the contact force is still bigger than 0.

During the first experiment, especially for softer materials, it is expected to see a certain relaxation and deformation of the surface. A force is brought onto the surface and the surface is expected to respond to this force in a way which is noticeable in the image.

With the second experiment the relation between the resolution of the images and the contact force is investigated directly. It is expected that the changes in resolution will be bigger for soft samples than for hard samples.

The samples chosen for these experiments are graphite (HOPG), mica (muscovite) and the 0.3 μm diamond film on (100) Silicon (further mentioned as the diamond sample). Compared to the samples used for measuring contact forces described in Chapter 4, the gold sample is replaced by the diamond sample. The reason for this change is that for this experiment the hardness of the surface of the sample is expected to be of influence in the relationship between resolution and contact force. To look at this influence it is preferred to look at samples with different hardnesses. According to the

CRC handbook of materials the hardness on the Moh's scale of the available samples (and tip) is:

graphite   0.5
mica   2.5-3
gold   2.5-3
siliconnitrate   9
diamond   10

Mica and gold have the same hardness, taking into account that on mica it is easier to get a clear image (depending on sample quality and material structure) the mica sample is chosen to take part into this experiment.

Due to the unavoidable use of large measuring forces the graphite and mica sample will deform while measuring. This will be made clear with the next calculation.. To get atomic resolution the contact area is in the order of magnitude of atoms (a contact radius in the order of magnitude of Angstoms), so a contact area of 10^{-20} m^2. Using a contact force in the order of magnitude of 10^{-8} N, the pressure on the sample will be 10^{12} Pa. Taking into account that the compressive strength of graphite $5.9*10^6$ Pa is, it can be concluded that the graphite will deform while it is measured. For mica it was not possible to find the compressive strength, but because it has a layered structure just as graphite and it's hardness on Moh's scale relatively close to graphite it will not differ from the compressive strength of graphite more than a few orders of magnitude. So the mica sample won't resist and will deform while measuring. For Siliconnitrate the compressive strength is $1.5*10^{13}$ Pa, so it will resist against deformation. The compressive strength of diamond is $2.2*10^{14}$ Pa, so diamond will also resist the pressure caused by the measuring force.

6.2 Results and analysis

Before going into detail for the specific samples in separate sub paragraphs, first a general effect for all the samples will be described.

The results of the first experiment for all the samples showed that the force curve as a whole was moving down in the graph. This means that the (A-B)/(A+B)-signal is increasing while time passes. This signal is increasing when the light of the laserbeam is falling in on the photodiode on a lower part. This can be caused by a thermal effect, which we will discuss roughly.
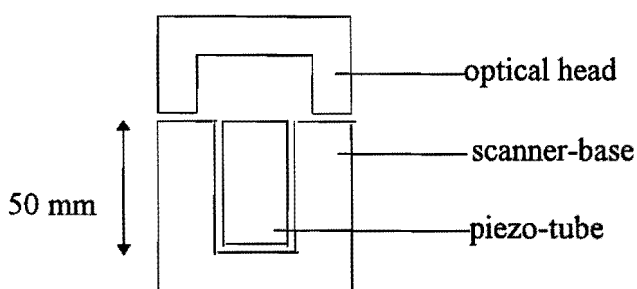Figure 6.1 shows a model of the upperhalf of the nanoscope II.

Figure 6. 1

The head of the Nanoscope II is made of invar and the housing of the scanner is made of steel. According to the polytechnisch zakboekje the linear coefficient of expansion of steel is $10*10^{-6}$ 1/°C, and the one of invar is $1*10^{-6}$ 1/°C. This difference in coefficient of expansion makes that invar is assumed temperature invariant. The temperature of the room in which all the experiments are executed is kept stable on 20° C±1° C. While executing an experiment there is a light pointed on the head and the base, so they will be heated . Assuming an ideal roomtemperature control, the temperature of the base can rise with one degree, which means that the head with cantilever is moved up $50*10^{-3} * 10*10^{-6} = 500*10^{-9}$ m = 500 nm relatively to the sample. While the cantilever is moved up due to this expansion it has to bent down to the sample more to stay in contact. This causes an increasing of the (A-B)/(A+B)-signal during the whole force curve, so the curve is moving down in it's graph as mentioned above.

6.2.1 Graphite

The images made during the first experiment (prints of two of the measurements are included in Appendix C page 44 and 45) and the second experiment (prints of three measurements are included in Appendix C page 46,47 and 48) show roughly the same pattern.
This pattern can be recognized as the three-for-hexagon pattern. Figure 6.2.a is showing the complete structure of graphite, the three-for-hexagon structure shown in the AFM-images can be understood by taking the geometry relaxation of the graphite surface into account.

Adjacent layers of highly ordered pyrolytic graphite (HOPG) are arranged in such a way that there occur two types of carbon atoms (A and B) on the surface layer, as shown in figure 6.2.b. The A-site carbon atoms lie directly above the carbon atoms of the underlying layer, and the B-site carbon atoms are located above the centers of the carbon hexagons of the underlying layer.
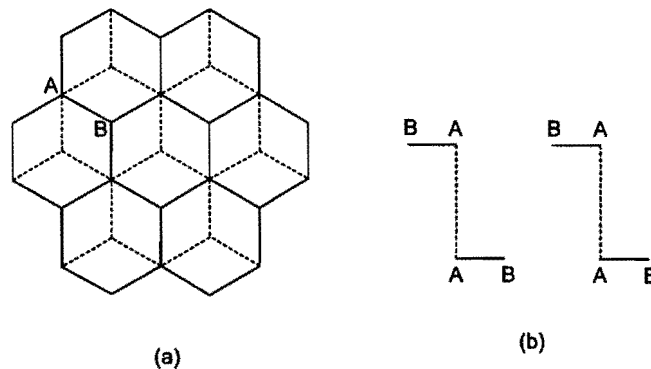

(a)   (b)

Figure 6. 2

Due to the interlayer interactions occurring through the A-site carbon atoms, the π-electron band levels of HOPG in the vicinity of e_f are more concentrated on the p_π - orbitals of the B-site carbon atoms than on those of the A-site carbon atoms (chapter 5

,14). Therefore, the total density plots ($\rho(e_f, r_0)$) for HOPG have a higher density on the B-site carbon atoms. STM and AFM images of HOPG obtained from simultaneous STM/AFM measurements have a three-for-hexagon pattern with an identical peak registry (Magonov). Consequently, the bright spots of the AFM images, which represent the regions of stronger tip-sample repulsive forces, coincide with those of the STM images.(the B-sites). This indicates that the tip force depresses the B-site atoms less than the A-site atoms. For an unrelaxed graphite surface monolayer, all carbon atoms should be seen with equal brightness in the AFM image. So, the atomic scale surface relaxation of HOPG induced by the tip force will be analyzed.

The local hardness of the A- and B-site in HOPG can be estimated using the atom-atom potential [20]:

$$E = -Ar^{-6} + B\exp(-Cr)$$

for a nonbonded C-C contact of distance r, where A=2377 Å^6 kJ/mol, B=349.90 kJ/mol and C=3.60 Å^{-1}. This potential reproduces the interlayer distance of 3.35 Å in bulk HOPG. For simplicity, the local hardness of the A- and B-sites in the surface graphite monolayer is estimated on the basis of a graphite bilayer, because what matters eventually for STM and AFM imaging is the atomic-scale topography change in the surface layer. Here the main concern is the microscopic relaxation of the surface monolayer, whether or not the B-site carbons are depressed less than the A-site carbons. Therefore, the geometry of the bottom sheet of the graphite bilayer can be assumed to be frozen.

Interesting quantities to calculate are the energies $\Delta E_{A,0}$ and $\Delta E_{B,0}$ needed to depress the surface carbon atoms at the A- and B-sites, respectively, by Δz_0 toward the underlying layer while keeping all remaining carbon atom positions fixed (14). These values calculated as a function of Δz_0 are summarized in table 6.1, and reveal that for a given amount of energy supplied, the B-site carbon can be depressed more than the A-site carbon.

Δz_0 (Å)	$\Delta E_{A,0}$ (kJ/mol)	$\Delta E_{B,0}$ (kJ/mol)
0.1	0.54	0.37
0.2	1.67	1.21
0.3	3.64	2.72
0.4	6.74	5.15
0.5	11.59	8.91

Table 6. 1

To achieve the same extent of depression, the A-site requires more energy, and is therefore harder, than the B-site. Given the fact that the A-site atoms have interlayer C-C interactions while the B-site atoms do not, this finding is reasonable but contradicts the conclusion from the simultaneous STM/AFM study. This problem stems from the implicit assumption of the analysis, the treatment of the tip as a mathematical point tip.
In a graphite sheet all carbon atoms are linked by the C-C bond network, and the stretching of the C-C bond raises its energy. Thus, depression of one carbon atom (directly under the tip atom) by Δz_0 will induce that of its three first-nearest-neighbor

(FNN) carbon atoms by Δz_1, that of its six-second-nearest neighbor (SNN) carbon atoms by Δz_2, and so on. Eventually this leads to a circular depression under the tip atom. The C-C bond length of the graphite layer is not large compared with the atomic radii of the tipatoms. Therefore, even for the most ideal case when the tip apex is given by a single atom, the depression effect of the tip force must be strongly felt by the four adjacent carbon atoms, namely the carbon atom lying directly under the tip atom plus the three FNN carbon atoms ($\Delta z_0 \approx \Delta z_1 > \Delta z_2 > ...$). On the basis of a graphite bilayer, one can calculate the energy $\Delta E_{A,1}$ needed to depress an A-site atom of the surface monolayer by Δz_0 and its three FNN B-site atoms by Δz_1, with the positions of all other atoms frozen, for several values of the ratio $\Delta z_1/\Delta z_0$. Likewise, one can calculate $\Delta E_{B,1}$ needed to depress a B-site atom of the surface monolayer by Δz_0 and its three FNN A-site atoms by Δz_1. Figure 6.3 plots the relative energy $\Delta\Delta E_1 = \Delta E_{B,1} - \Delta E_{A,1}$ calculated as a function of $\Delta z_1/\Delta z_0$ for $\Delta z_0 = 0.3$ Å.
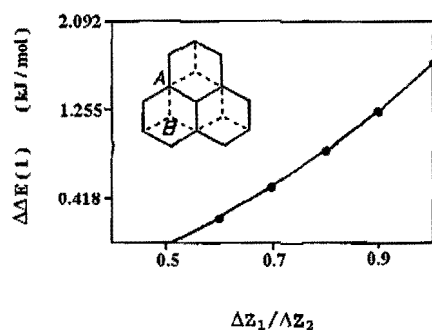

Figure 6. 3

Because the C-C bond length and the tip-atom radius are comparable, the ratio $\Delta z_1/\Delta z_0$ should be close to unity. Therefore, the plot of figure 6.3 shows that the B-site is more difficult to depress than the A-site ($\Delta\Delta E_1 > 0$). So, this explains the three-for-hexagon pattern of the AFM image.

The distances between the centers of two atoms in the measured images is between 2.5 and 3.3 Å. These measurements are in agreement with theory, because the bondlength between two carbon atoms is about 3 Å.

1:     During the first experiment, several times the graphite sample was imaged for about one hour. The contact forces corresponding to the images are listed next to the images included in Appendix C, page 44 and 45. The contact force is ranging from 40.05 nN to 46.92 nN and from 77.3 nN to 94.9 nN, which can be considered as a stable contact force, taking into account all the disturbing influences from the environment. The magnitude of the forces are depending on the snap into contact. The images all seem to have the same resolution.

2:     This experiment was also executed for several times. During the here reported ones, the setpoint was changed from 0 to -5 V. This was the maximum range in which it still was possible to calculate the contact force from the force curve. The contact forces corresponding with the images are listed next to these images included in appendix C, page 46, 47 and 48.

Over all the different series of measurements, the force is varied from 84.6 nN to 9.6 nN. Comparing all the measurements with each other, it can only be concluded that a contact force smaller than 30 nN gives images in which it is not possible to distinguish separate carbon atoms. So the imaging force has to be bigger than 30 nN to get a clear image from the surface in ambient conditions. The rest of the images all have about the same resolution, though these images are made with forces ranging from 30 nN to 85 nN. It is obvious that imaging taken with a contact force of 35 nN will show a less deformed surface with less contrast between the hard and the softer parts, than an image taken with a contact force of 85 nN, but this difference can not be seen comparing the measurements of this experiment. The problem is that the range in which the force can be changed on the Nanoscope II is too small to notice these differences.

6.2.2 Mica

The images made during the first experiment (prints of two of the measurements are included in Appendix D page 49 and 50) and the second experiment (prints of three measurements are included in Appendix D page 51, 52 and 53) show the same pattern. This pattern shows the mica structure.

Mica is a layered material consisting of negatively charged 2:1 layers that are compensated and bonded together by large, positively charged, interlayer cations. A 2:1 layer contains two tetrahedral sheets and one octahedral sheet. Each tetrahedral sheet is of composition T_2O_5 (T=tetrahedral cation), and within each sheet tetrahedra are linked with neighboring tetrahedra by sharing three corners each (the basal oxygens) to form an hexagonal mesh pattern of the sort illustrated in figure 6.4.a. The fourth tetrahedral corner (the apical oxygen) points in a direction normal to the sheet and at the same time forms part of an immediatly adjacent octahedral sheet in which individual octahedra are linked laterally by sharing octahedral edges as shown in figure 6.4.b. In a 2:1 layer the upper and lower planes of anions that comprise an octahedral sheet are also the common planes of junction with two oppositely directed tetrahedral sheets, as in figure 6.4.c.

● = Tetrahedral cation   O = Oxygen
● = Octahedral cation   ⊖ = Oxygen + Hydroxyl (in projection)

34
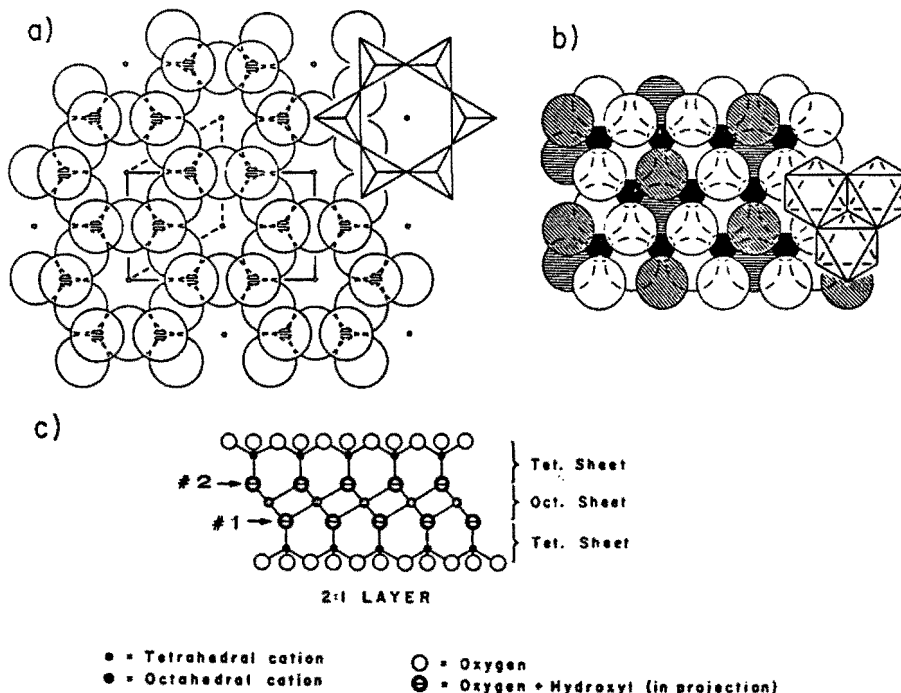
These planes of junction consist of the shared apical oxygens plus unshared OH groups that lie at the center of each tetrahedral six-fold ring at the same z-level as the apical oxygens. Fluorine may substitute for OH.

The mica sample used for this report is muscovite, $KAl_2(Si_3Al)O_{10}(OH,F)_2$. In this mica the tetrahedral cations are Si , the interlayer cations are K and the octahedral cations are Al.

On forehand it is expected to see the structure as shown above in figure 6.4.a. In the images, though a regular pattern is shown, the expected six-fold ring can not easily be recognized. In some images , for example images 3 and 5 in the first serie, it seems that 3 white 'balls' are connected together, and form a honeycomb, so you can recognize a honeycomb-pattern. The honeycomb then has a size of approximately 6.5 Å, which is close to the theoretical 5.2 Å when it is taken into account that because of the big measuring force the mica is deformed, which probably can mean stretched out.

The biggest problem with this explanation is, why only three pronounced white 'balls', and not six, which could mean that they represent the tetrahedra.

1:      During the first experiment, several times the mica sample was imaged for about one hour. The contact forces corresponding to the images are listed next to the images included in Appendix D, page 49 and 50. The corresponding contact forces are listed next to the images. The force is ranging from 71.71 nN to 82.69 nN and from 17.88 nN to 30.43 nN. For the first serie the force can be considered constant. The images of this serie all look very similar. The sample surface doesn't seem to change after imaging for an hour. For the second serie absolutely the forces are not varying much more than during the first serie, but relatively it is noticed that within the serie the force is redoubled, so we can't consider the force constant during the whole serie of measurements. This is also seen in the change of clearness of the images, compared to the first serie these changes are quiet big. That these changes are not due to the long imaging time can be concluded because the last image, made with a force 27.23 nN is again as clear as the first image.

2:      This experiment was also executed for several times. During the here reported ones, the setpoint was changed from 0 to -5 V. This was the maximum range in which it still was possible to calculate the contact force from the force curve. The results are included in Appendix D, page 51, 52 and 53. The contact forces corresponding with the images are listed next to these images.

Analyzing these results it is noticed that the images differ from brightness and clearness. In the last serie (p.53) the image made with a force of 36.65 nN starts to become vague, in the first serie (p.51) the image made with a force of 38.41 nN is still clear. So in ambient conditions clear images can be generated with a measuring force above approximately 36 nN. The upper limit is not found because the range in which the force can be varied is too small. That the force has to be this big is due to the waterlayer on the sample. When the force is in the order of 10^{-8} N the tip is able to go through the waterlayer and make an image of the surface, when the force is smaller the tip is not able to go through the waterlayer and therfore not reaching the surface.

6.2.3 Diamond

The analysis of the diamond results can not be as detailed as the ones about graphite and mica. On the diamond sample images of 2000x2000 nm, showing the diamond crystals, are made.

The diamond crystals looked at show no sharp endings in the image so probably not the diamond sample but the shape of the tip is imaged. To make this sure it is necessary to know more about the shape of the tip. Therefor the tip should have been examined under for example an electron microscope.

1:     During the first reported serie of measurements, though it is tried to keep the measuring force constant it is changing a lot (from 30.54 nN to 61.08 nN) probably due to changes in environment. This can be seen in appendix E, page 54 and 55. There are not significant changes in clearness. During the second serie the force is varying from 55.26 nN to 67.55 nN, which is considered as being constant. Here also there are not remarkable changes in clearness.

2:     With the diamond sample it was almost impossible to execute the second experiment. Results are shown in appendix E, page 56, 57 and 58. Changing the measurement force is almost impossible. When trying to lower the force under a magnitude of 40 nN their was no image at all, the screen became all black as if the tip was not making any contact with the sample

## 6.3 conclusions and recommendations

All the information presented in this chapter leads to a few general conclusions and recommendations.

- Due to the unavoidable use of large measuring forces the graphite and mica sample deform while measuring. The diamond sample and the tip of Siliconnitrate are able to resist the pressure on the surface during measuring.(§6.1)
- Due to thermal expansion of the housing of the piezo-tube on which the head is mounted, in time the measured force curves move down on the graphs.(§6.2)
- In general measuring a long time (an hour) does not have noticeable impact on the images made of a graphite, mica or diamond sample with the same force.(§6.2)
- The structure showed in images made on graphite are quite obvious in agreement with the theory about the graphite structure. Concerning the structures shown in the images made on mica there are difficulties to bring them in agreement with the theoretical known structure of mica. The diamond crystals looked at show no sharp endings in the image so probably not the diamond sample but the shape of the tip is imaged. To make this sure it would be helpful to know more about the shape of the tip. This can be done by examining the tip of the cantilever before using under an electron microscope. Then more can be said about the resolution of the images, as far as the resolution is determined by the shape of the tip. It can also be useful to look at the tip after imaging to see if the shape, and if so how, is changed during scanning. (§6.2)
- To examine the relation between resolution and contact force better it is necessary to be able to vary the contact force in a larger range. This can be done by varying the setpoint over a larger range. (§6.2)

Appendix A

An AFM image shows atomic-scale features with accurate lattice spacing and symmetry but this is not the garantee of atomic resolution.

While making an AFM image several atoms on the tip interact simultaneously with several atoms on the sample. Each atom of the tip that participates in imaging 'sees' the sample as a periodic lattice. But because the atoms of the tip are in different lateral positions, the lattice that each atom sees is shifted from the lattice seen by it's neighbors.
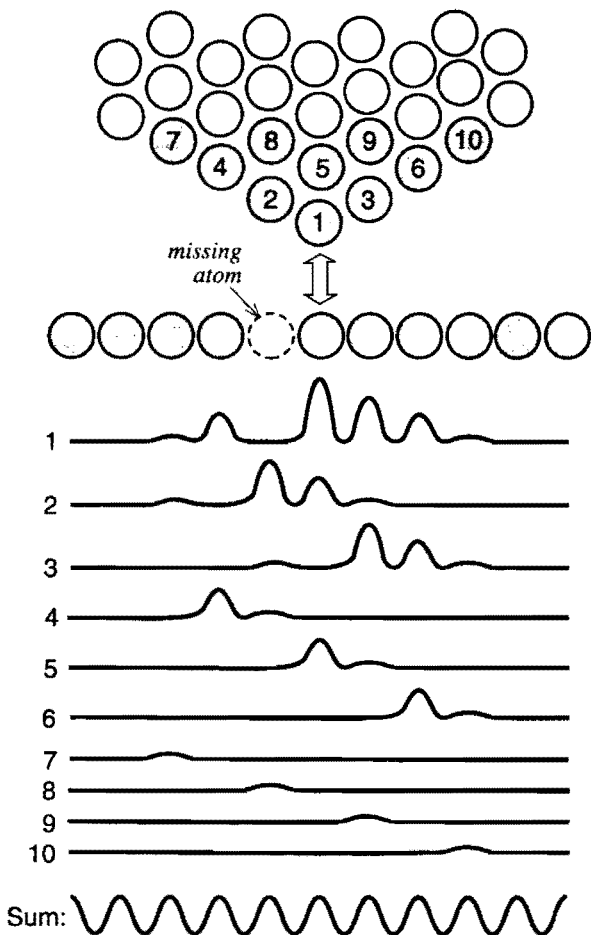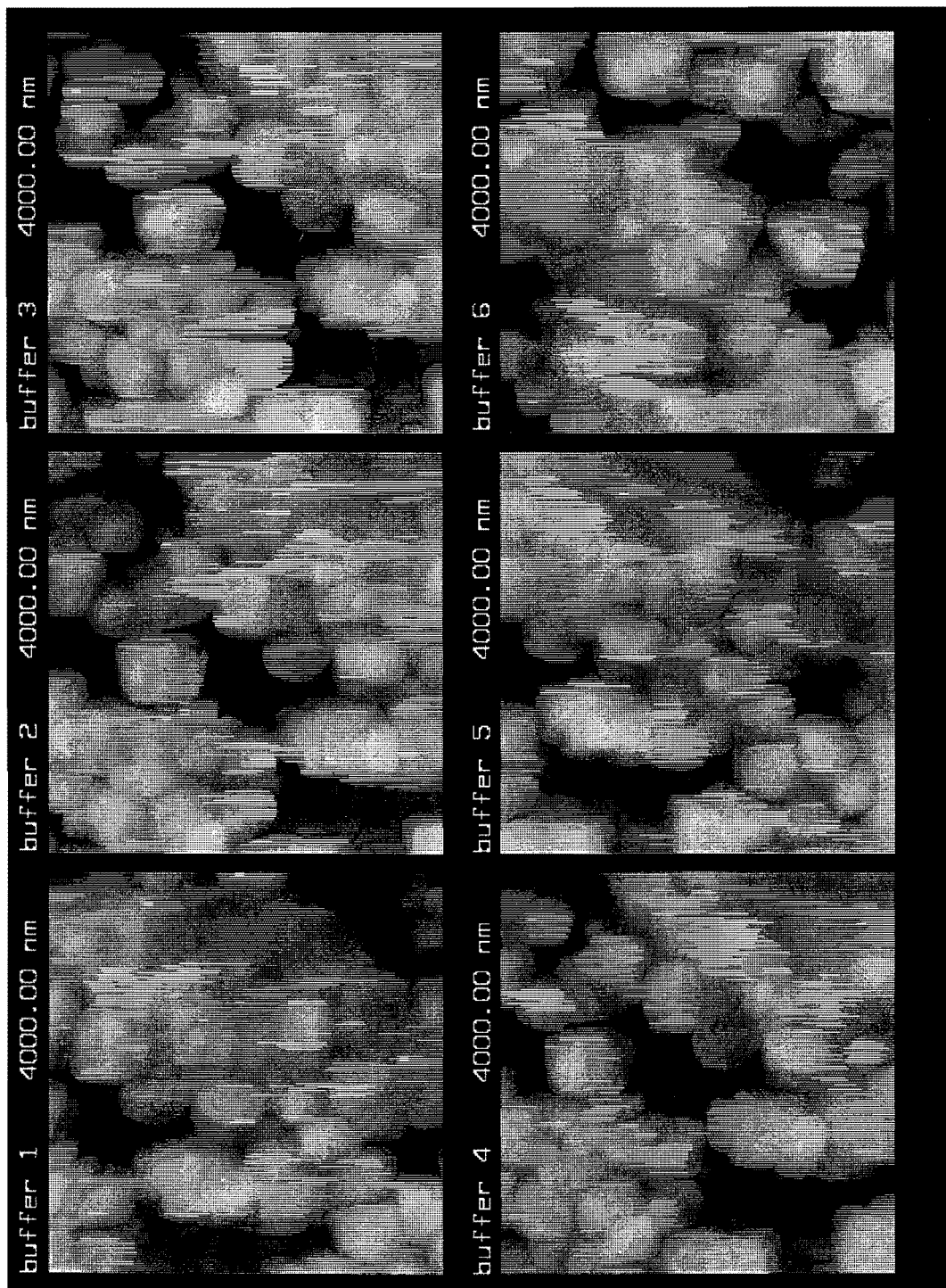

Each atom in the tip is also at a different height with respect to the sample. When the contributions from all of the participating atoms in the tip are combined at each snapshot in time, and the result is summed over time as the is scanned across in periodic surface, the final image is periodic with the correct symmetry and spacing.

However, if one atom were missing, the hole left behind would not be detected because the image represents a superposition of many images. For true atomic resolution, a single missing atom must be detectable.
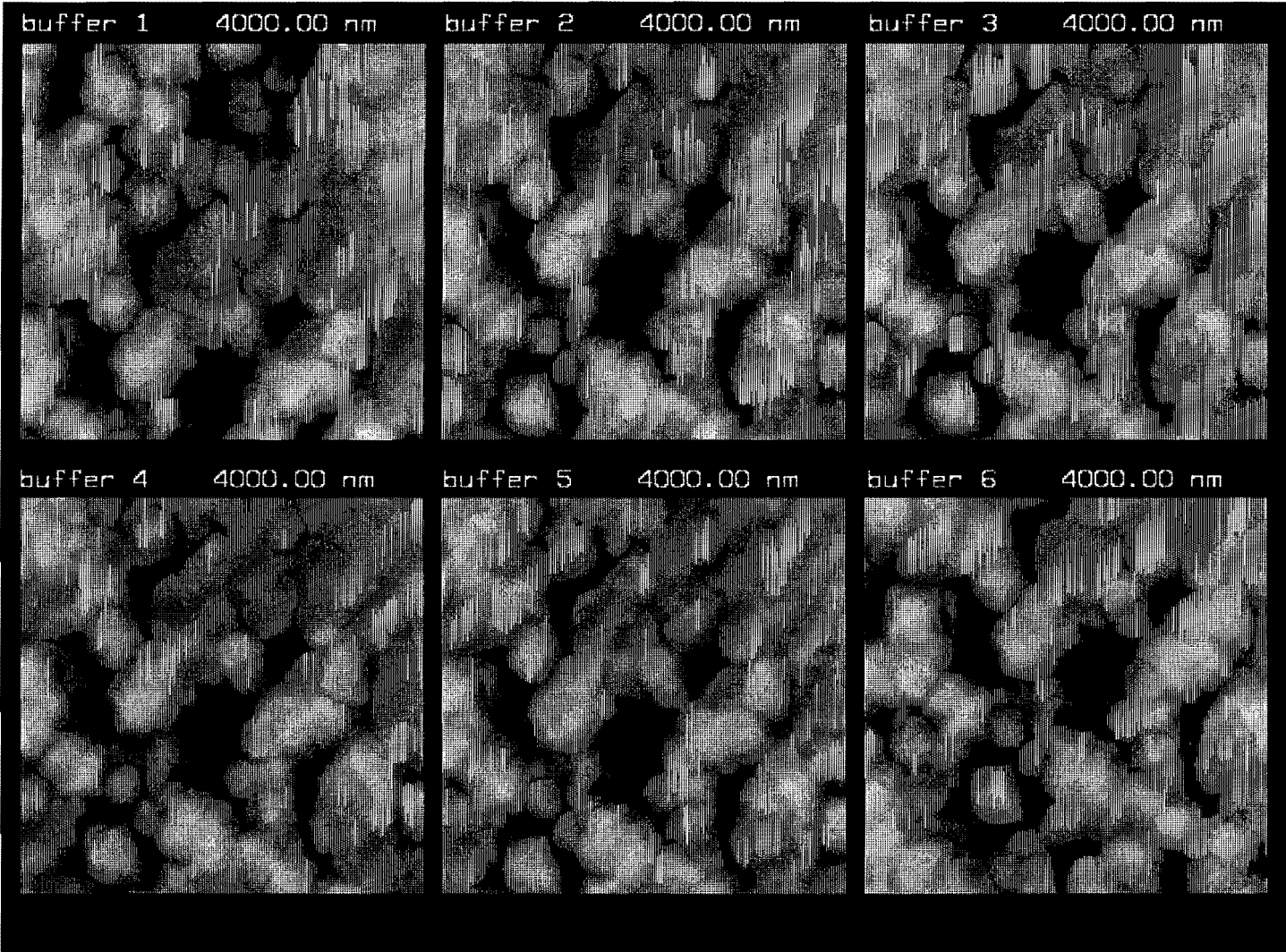
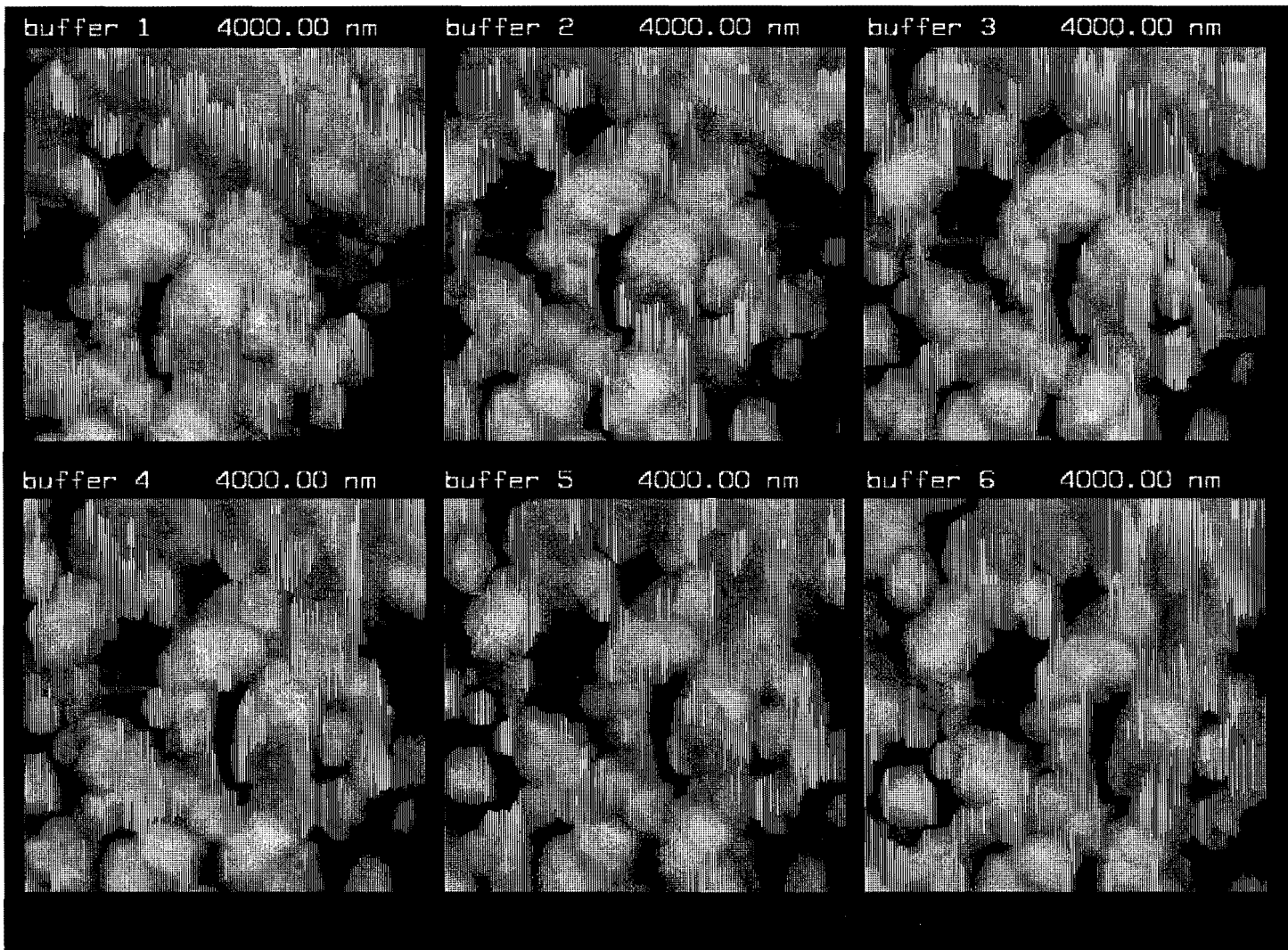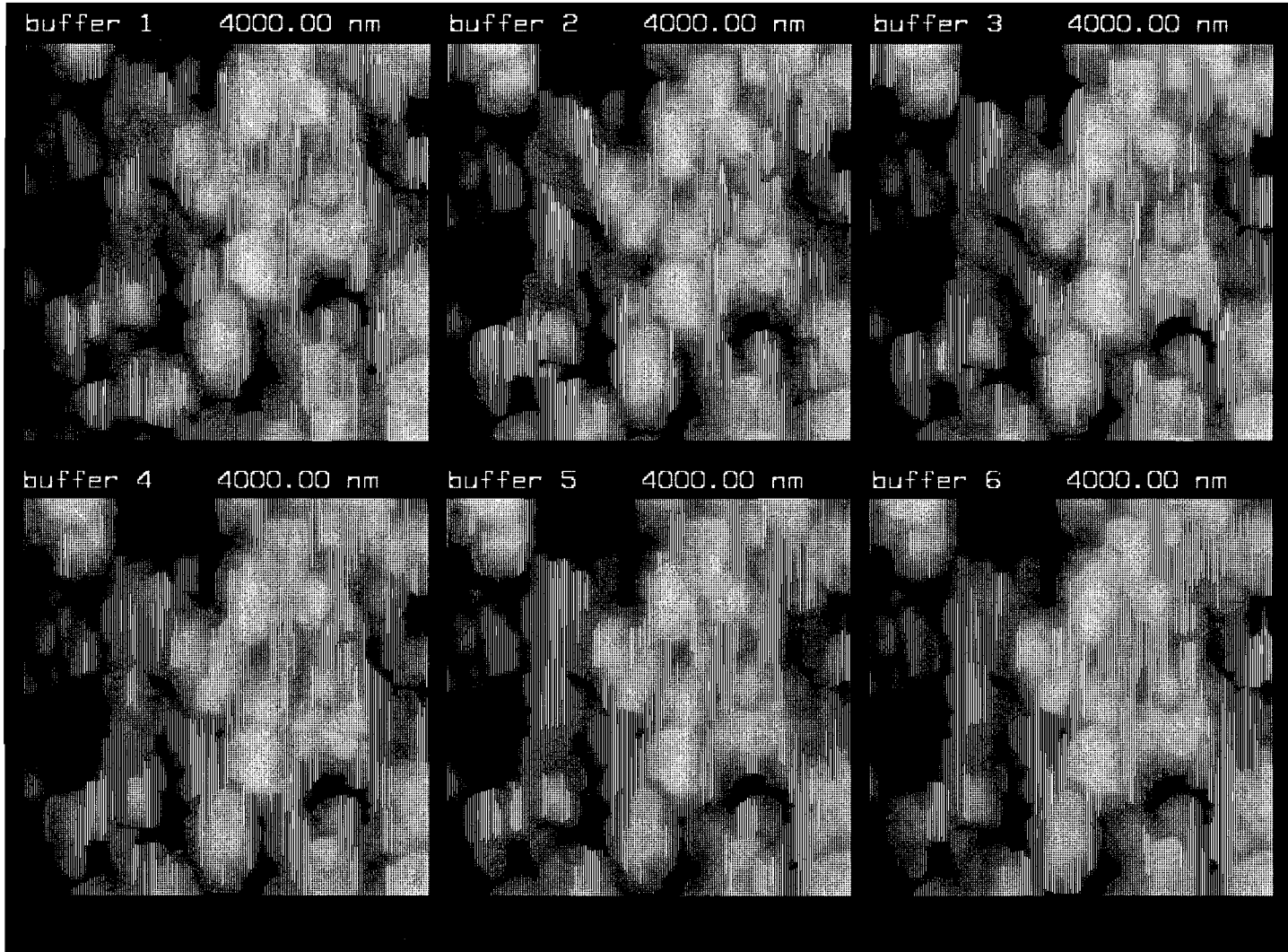Thus, generating an atomic-scale image of a periodic lattice, which is possible using contact AFM does not imply that true atomic resolution has been achieved. (1)

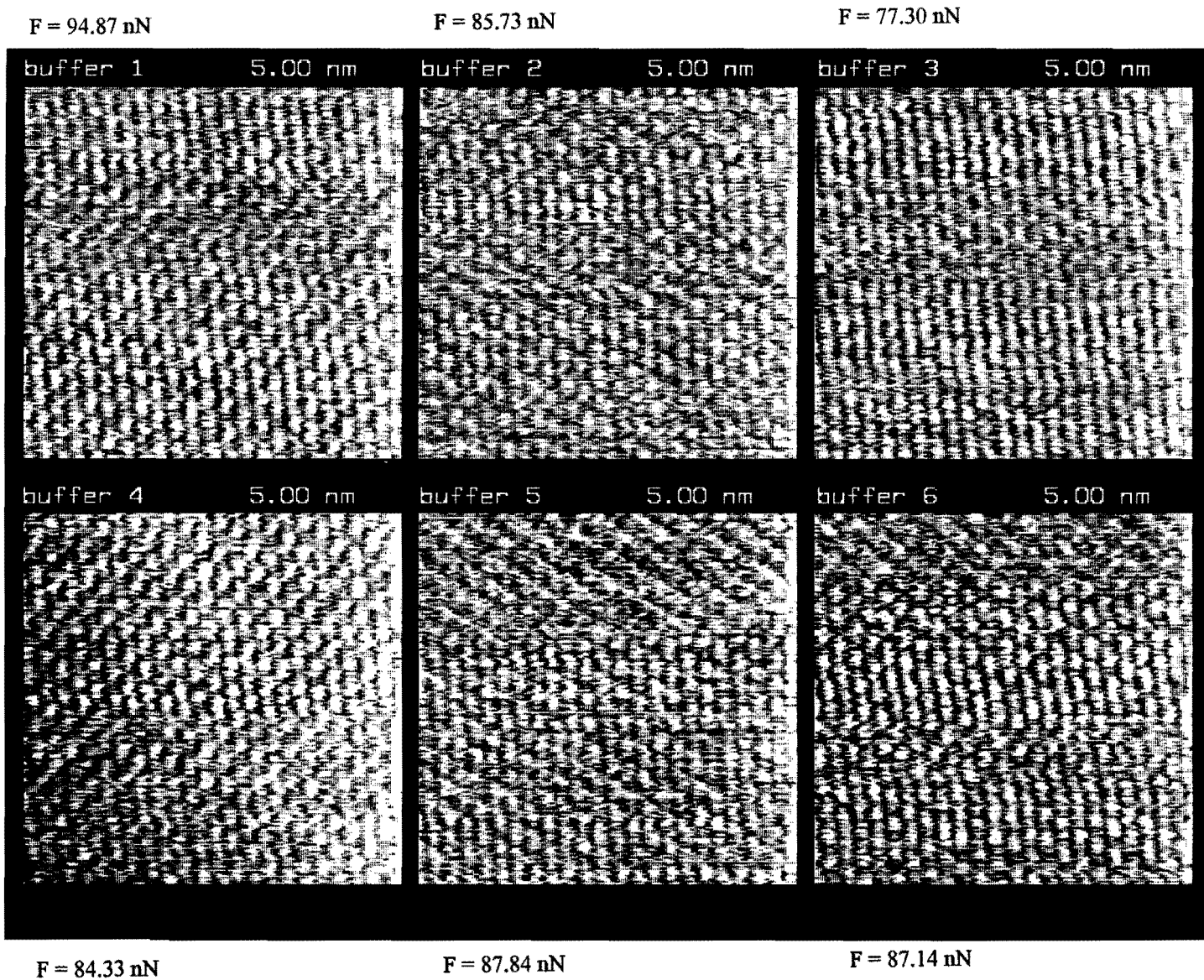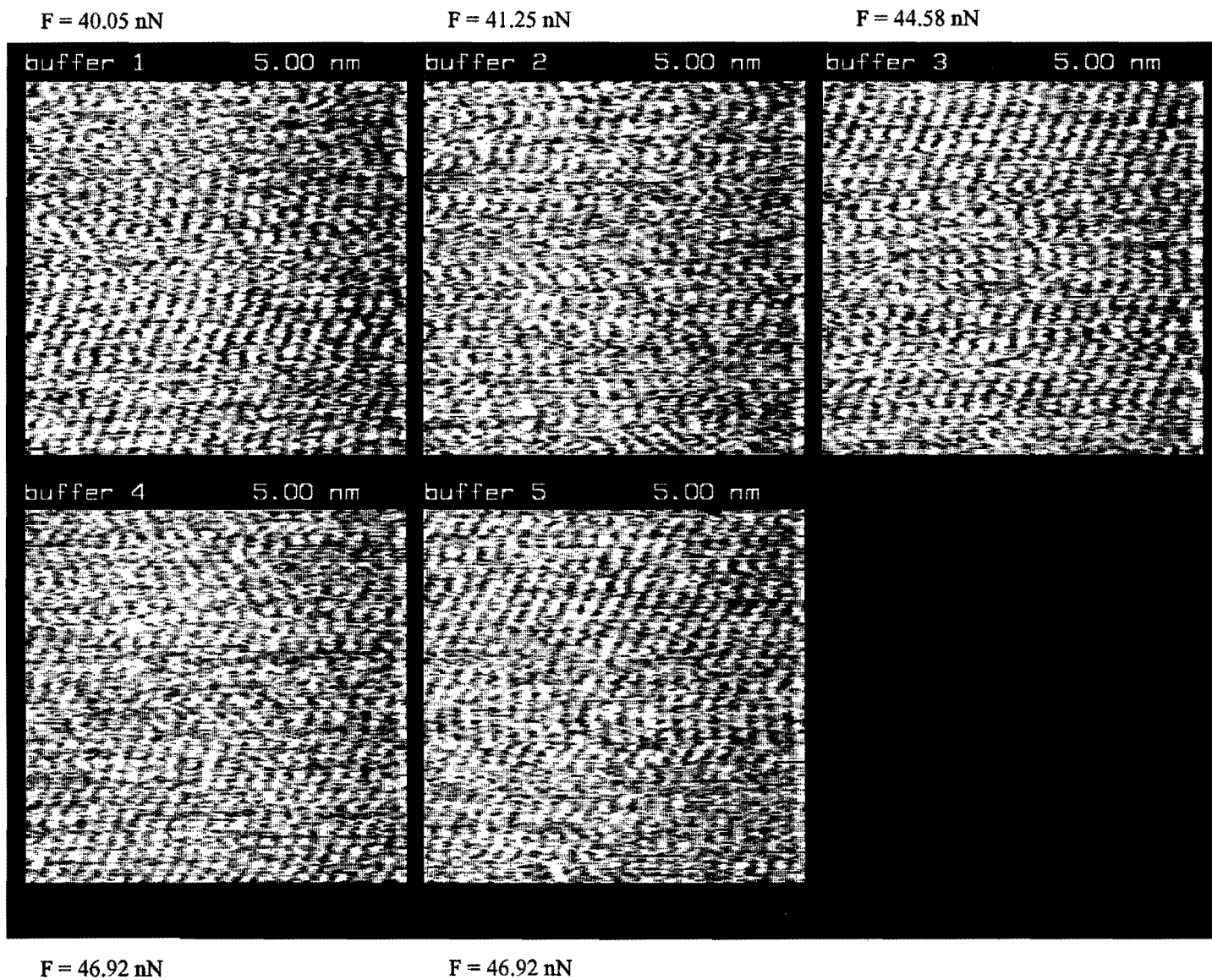# Appendix B

Diamond re-engagement experiment
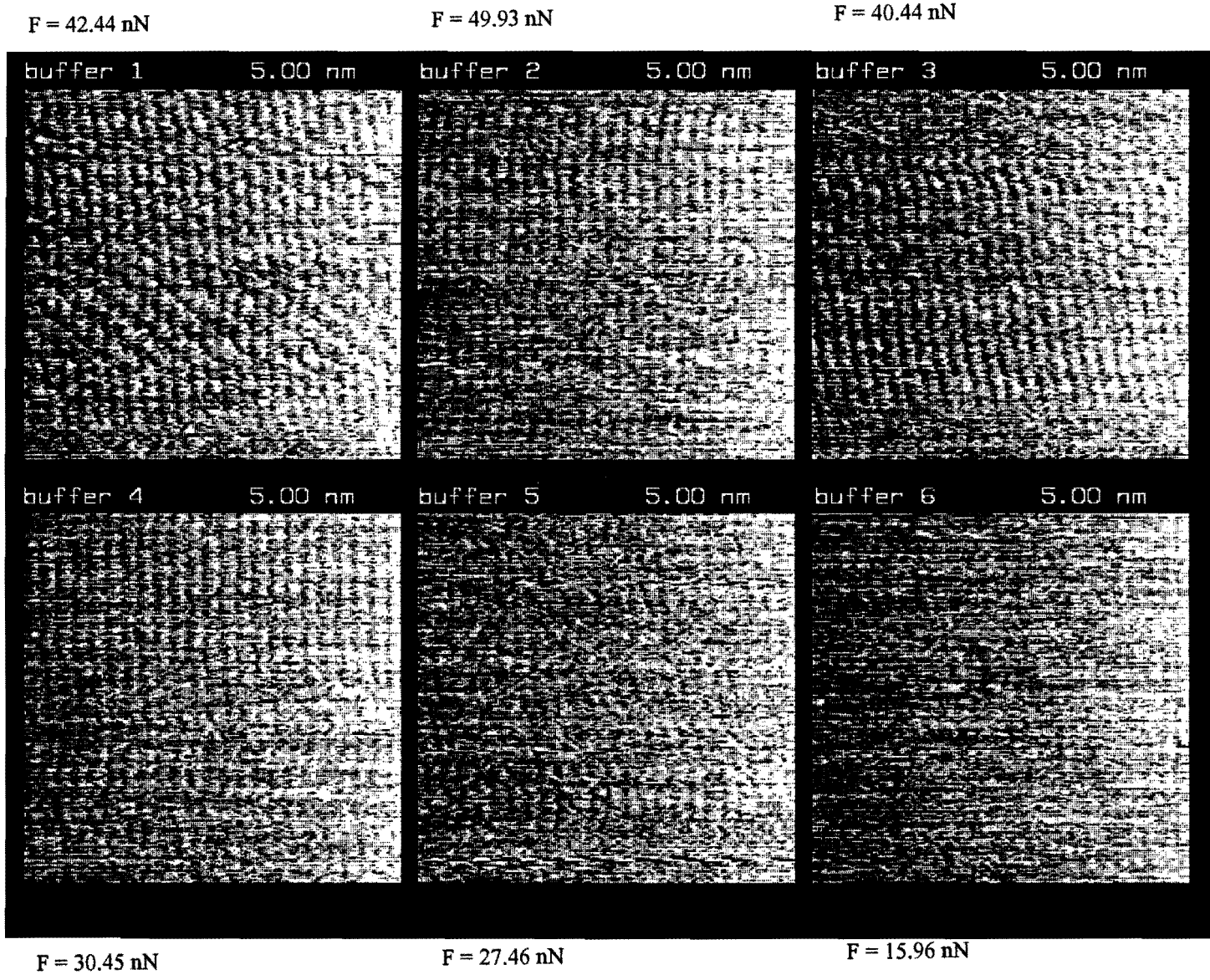
buffer 1   4000.00 nm   buffer 2   4000.00 nm   buffer 3   4000.00 nm

buffer 4   4000.00 nm   buffer 5   4000.00 nm   buffer 6   4000.00 nm

buffer 1   4000.00 nm   buffer 2   4000.00 nm   buffer 3   4000.00 nm

buffer 4   4000.00 nm   buffer 5   4000.00 nm   buffer 6   4000.00 nm
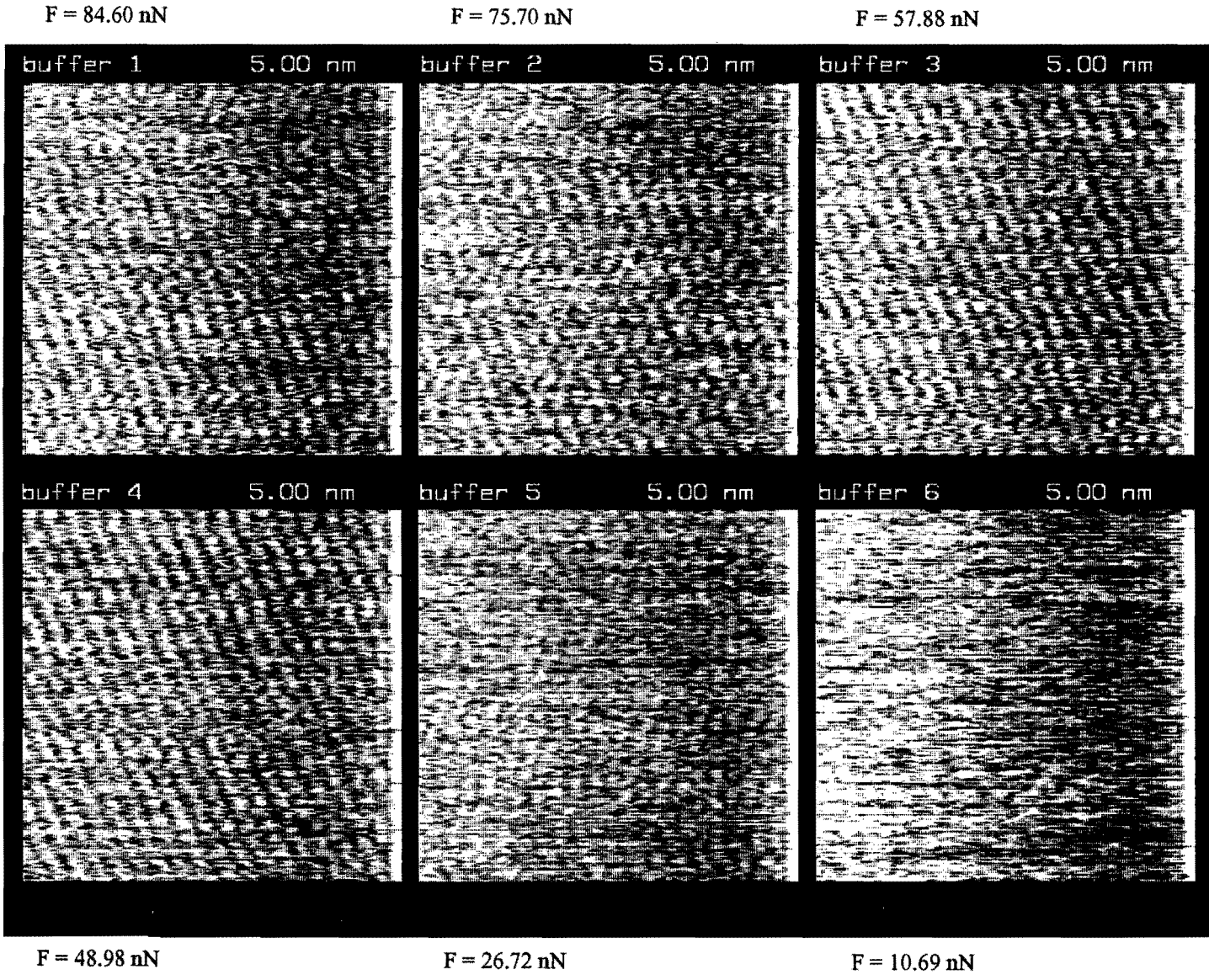
F = 94.87 nN   F = 85.73 nN   F = 77.30 nN

F = 84.33 nN   F = 87.84 nN   F = 87.14 nN
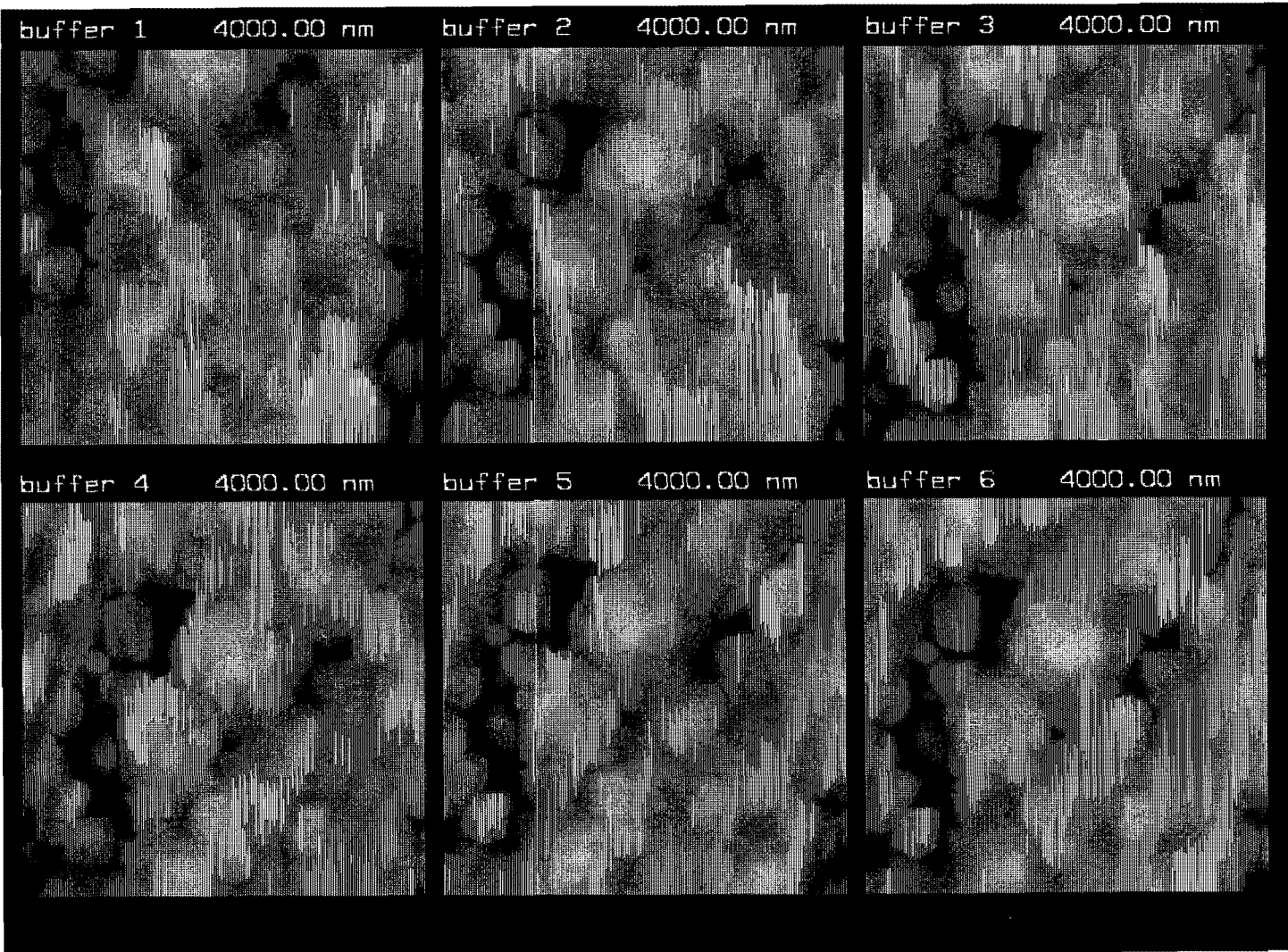
Graphite, constant force 2

44

F = 40.05 nN   F = 41.25 nN   F = 44.58 nN

F = 46.92 nN   F = 46.92 nN

F = 42.44 nN   F = 49.93 nN   F = 40.44 nN

F = 30.45 nN   F = 27.46 nN   F = 15.96 nN

45

F = 87.84 nN   F = 98.38 nN   F = 75.89 nN

F = 70.27 nN   F = 39.35 nN   F = 30.92 nN

F = 84.60 nN   F = 75.70 nN   F = 57.88 nN

F = 48.98 nN   F = 26.72 nN   F = 10.69 nN

F = 78.53 nN   F = 71.71 nN   F = 81.43 nN

F = 82.69 nN   F = 78.68 nN

F = 28.91 nN

F = 30.43 nN

F = 28.91 nN

F = 17.88 nN

F = 23.23 nN

F = 27.23 nN

F = 59.09 nN   F = 54.17 nN   F = 44.32 nN

F = 38.41 nN   F = 24.62 nN   F = 14.77 nN

F = 55.35 nN   F = 51.98 nN   F = 42.35 nN

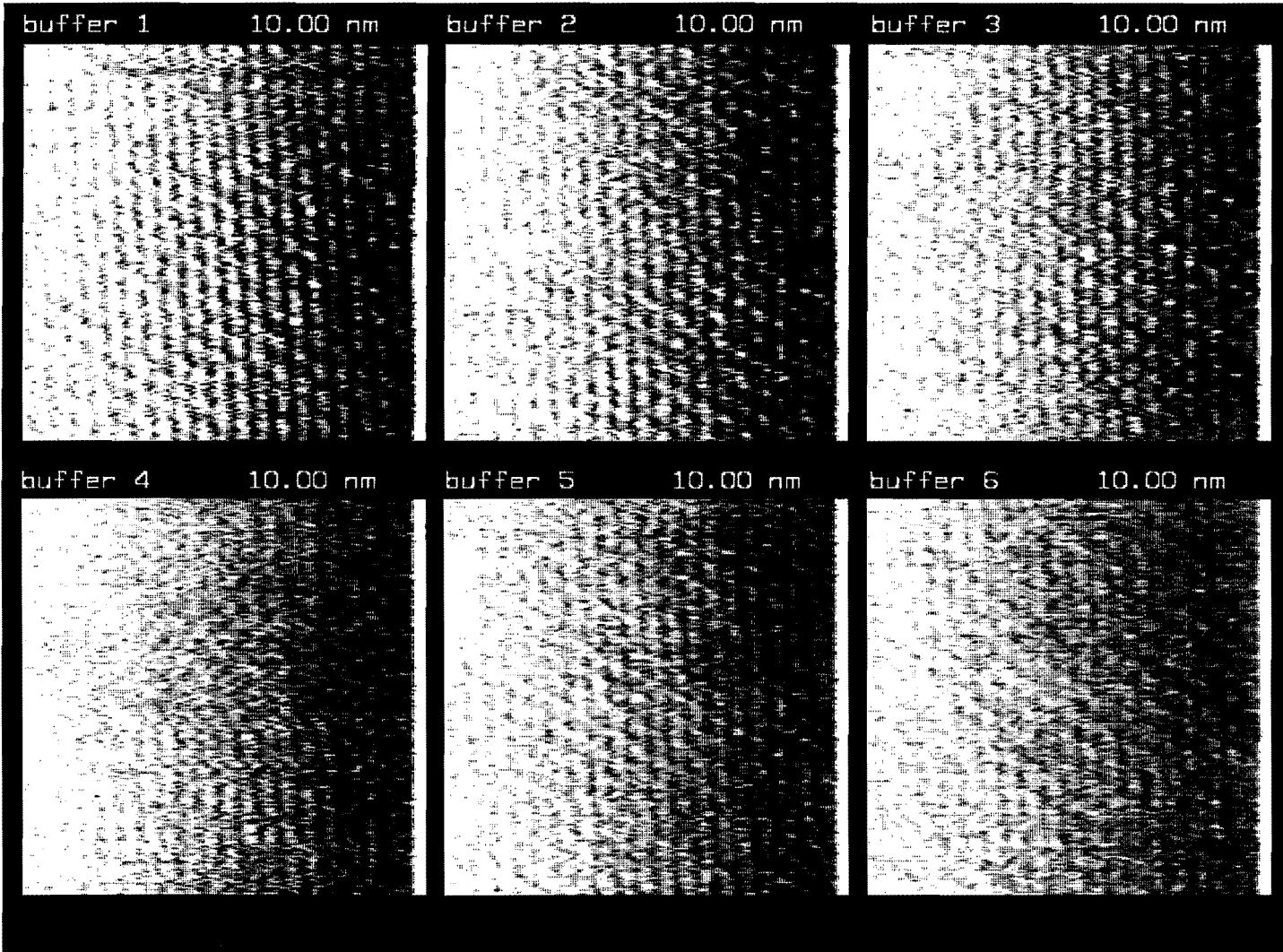Mica, varying force 2

51

F = 33.69 nN   F = 19.25 nN   F = 7.22 nN
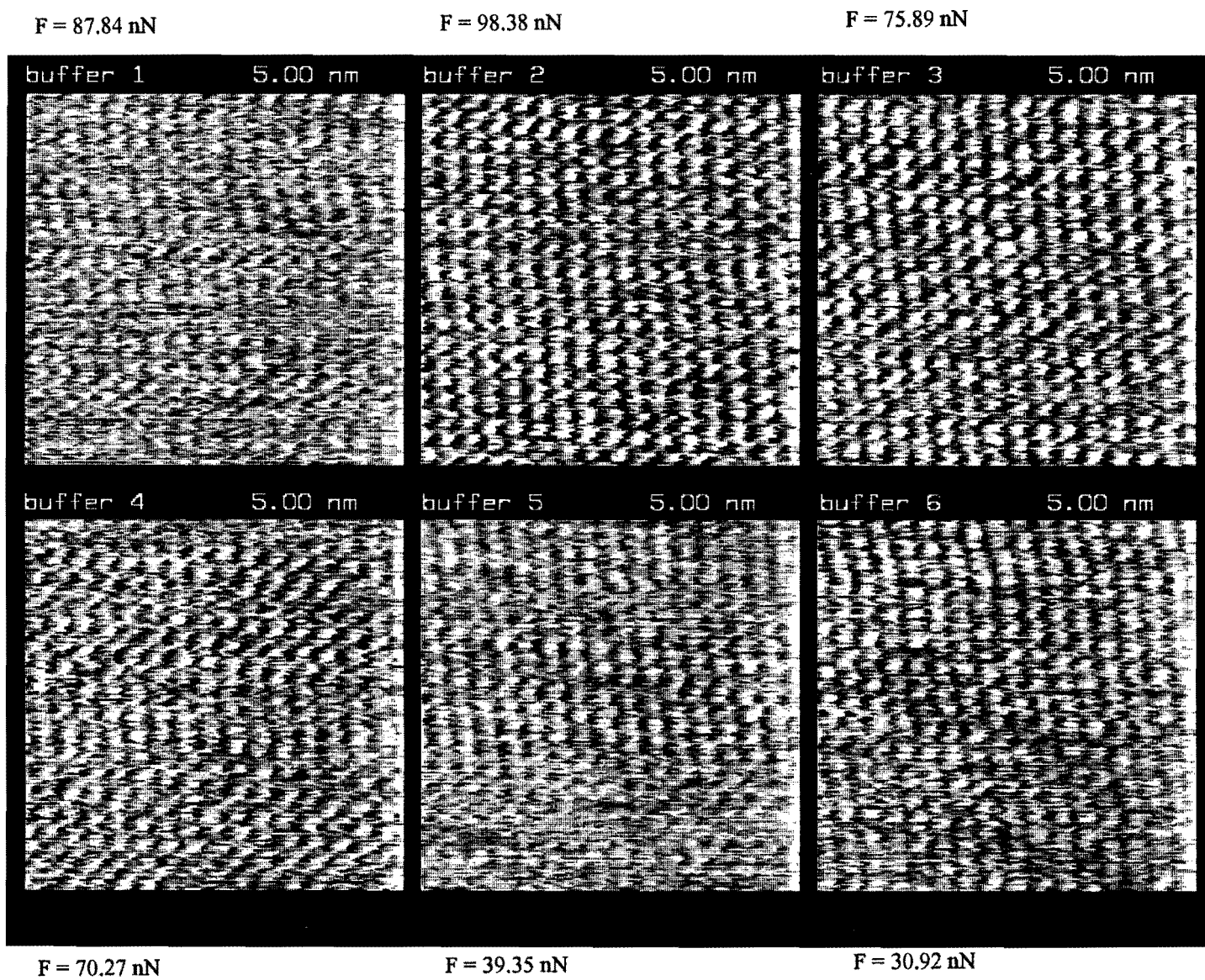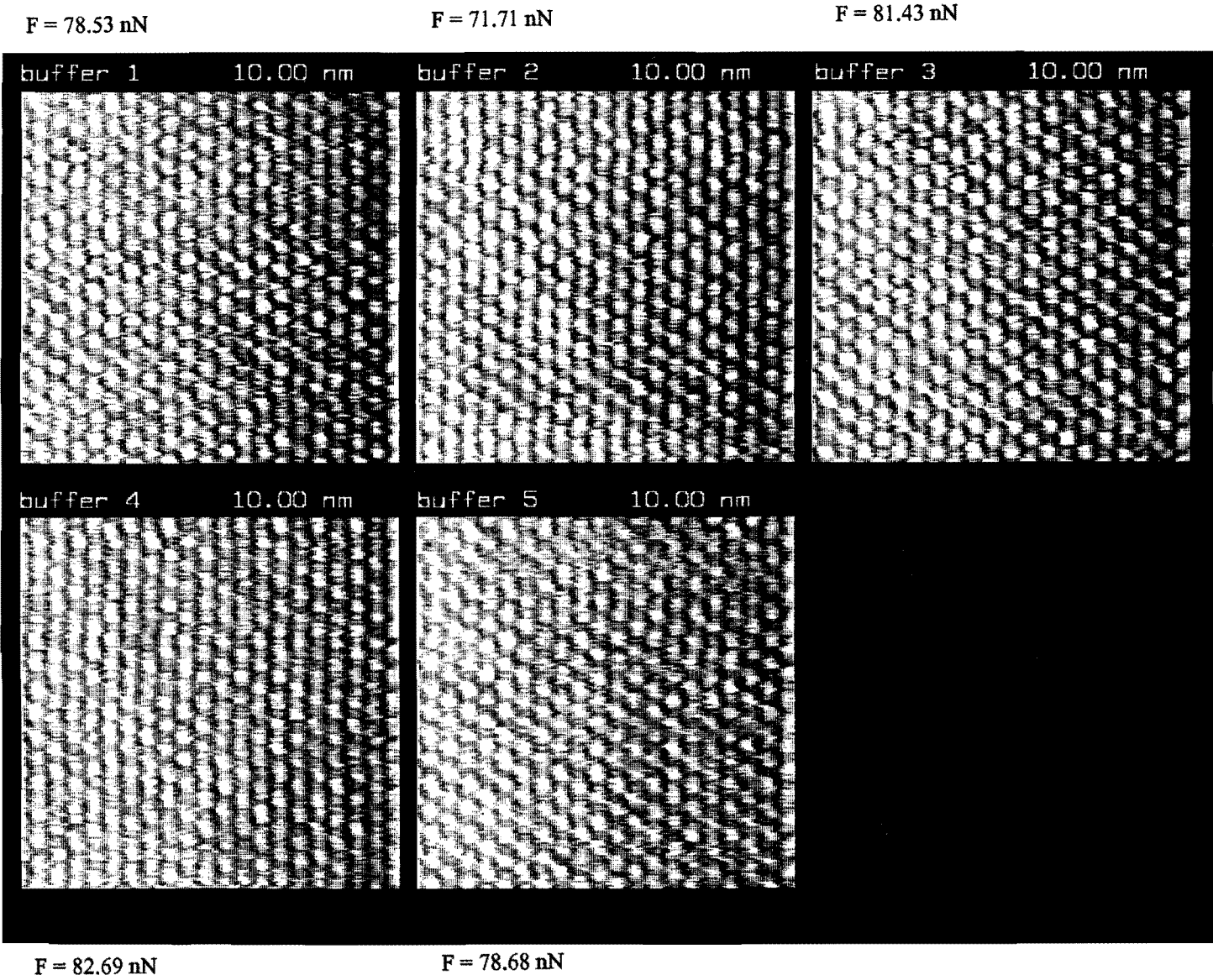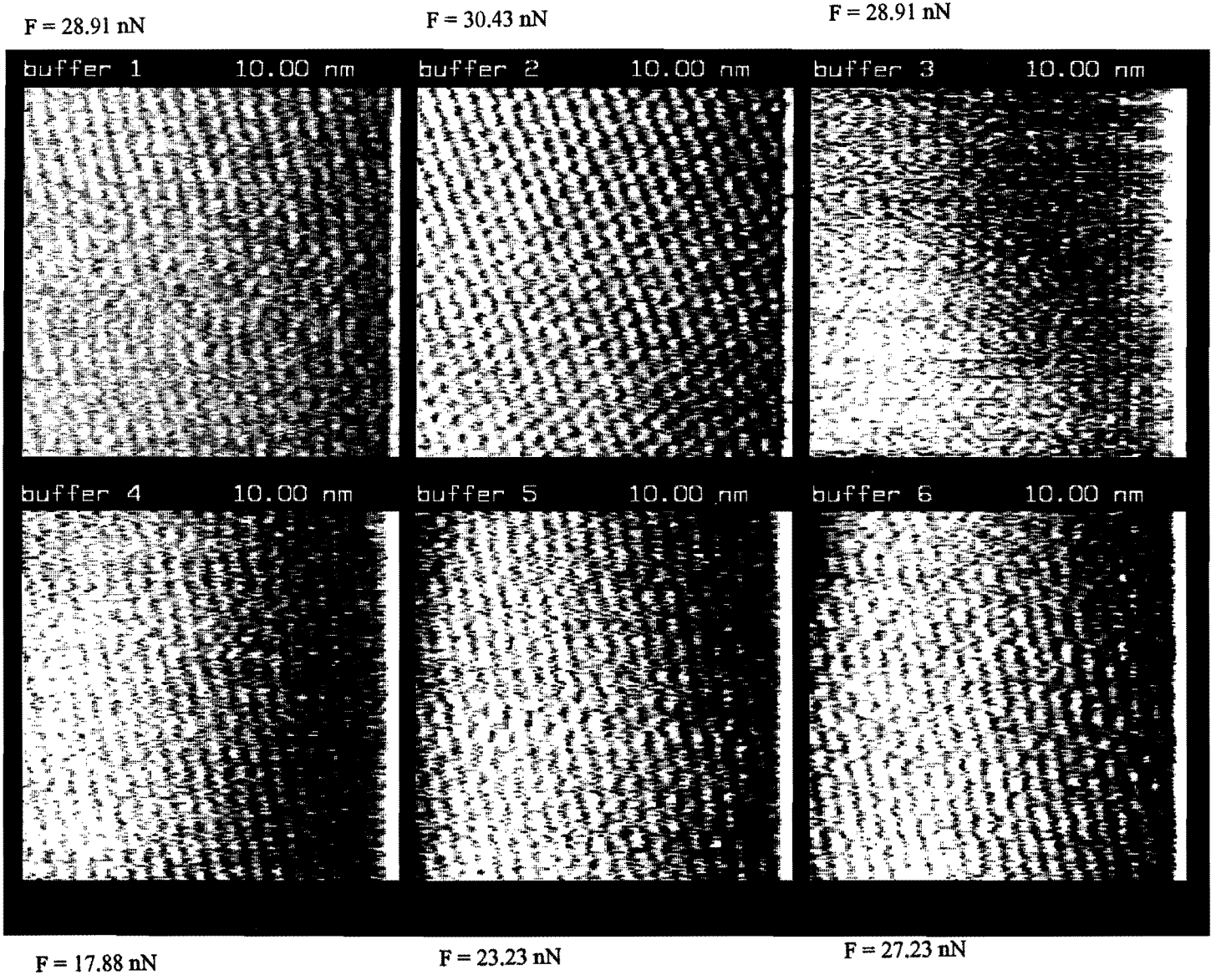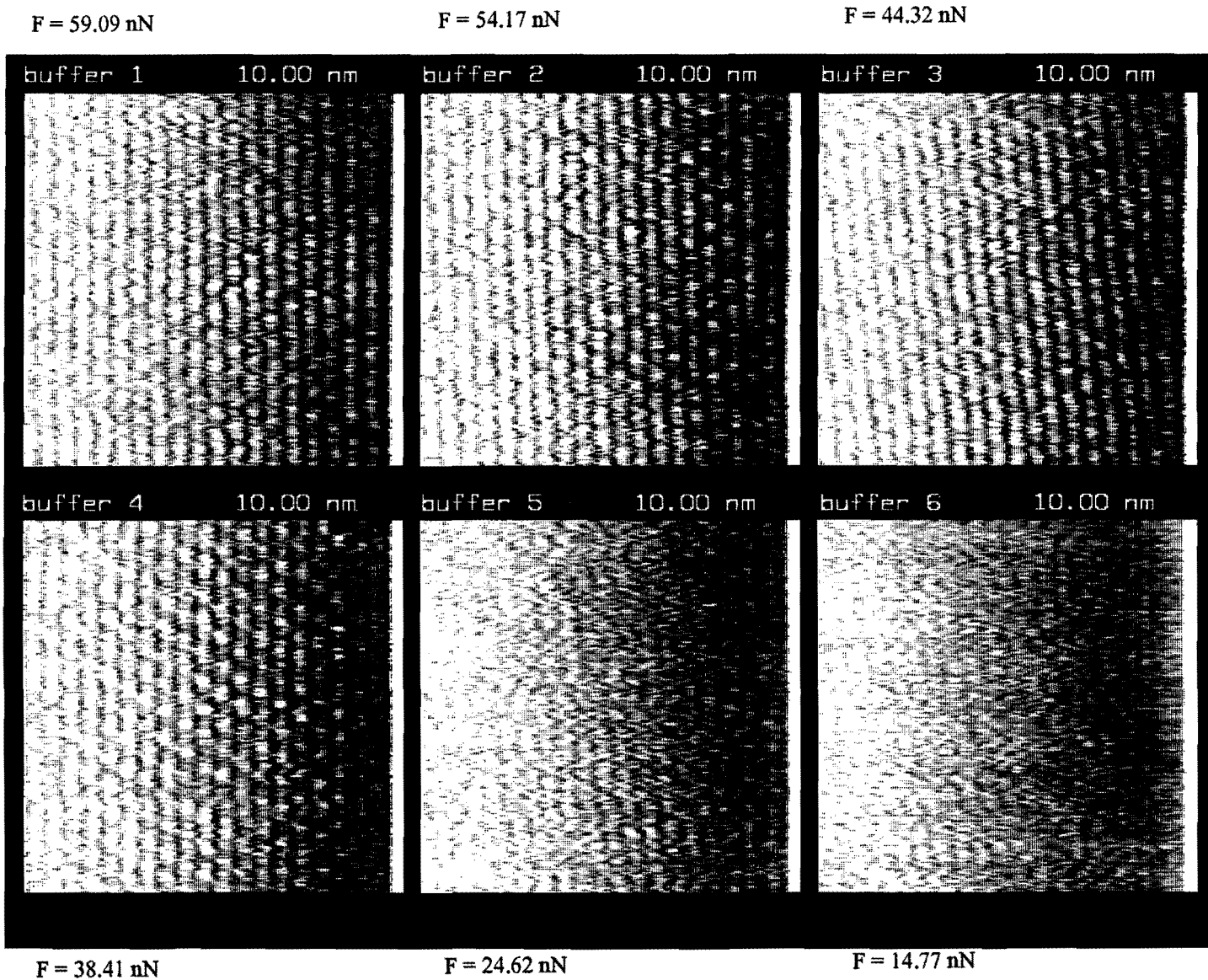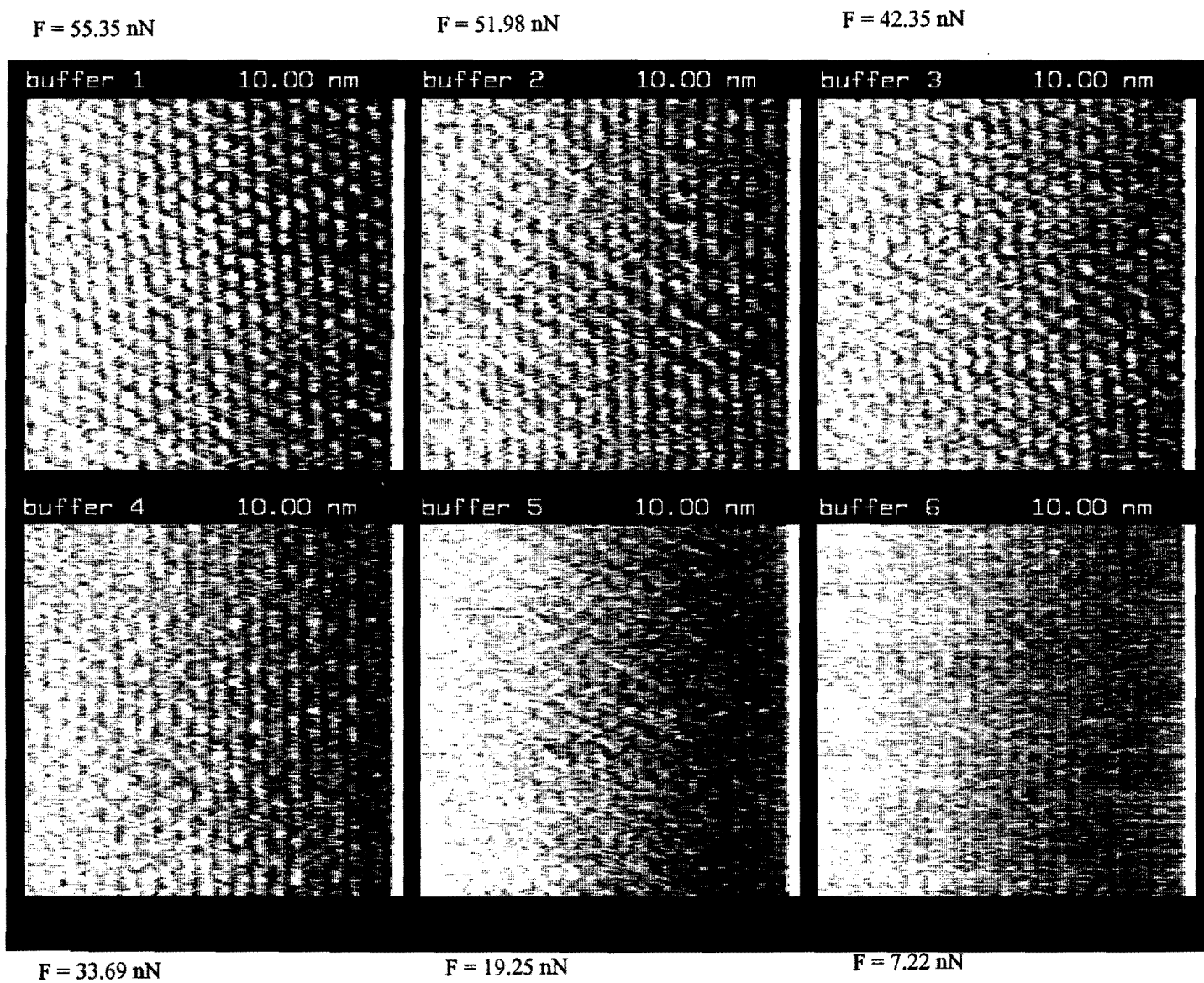
F = 65.74 nN

F = 55.78 nN

F = 47.01 nN

F = 36.65 nN
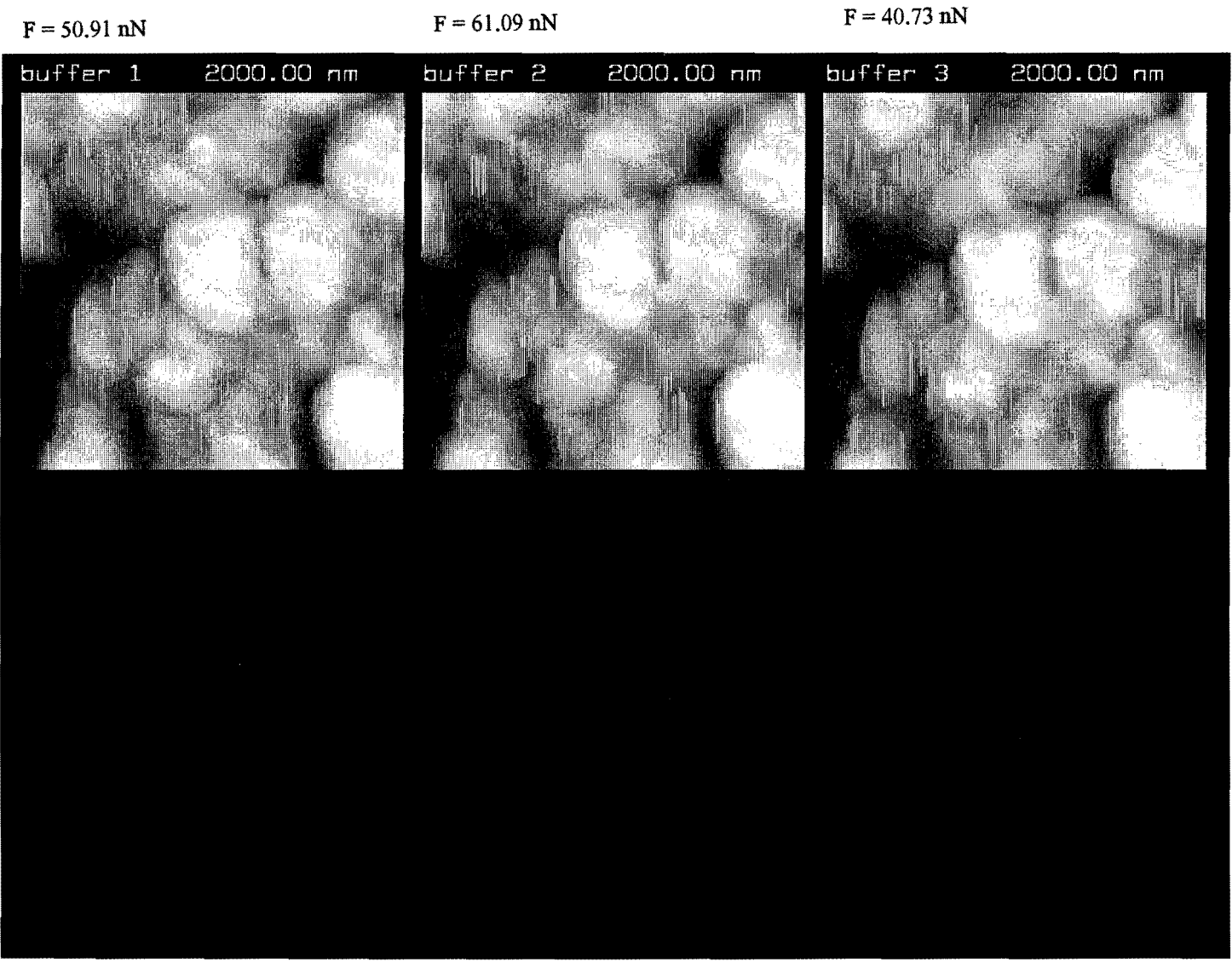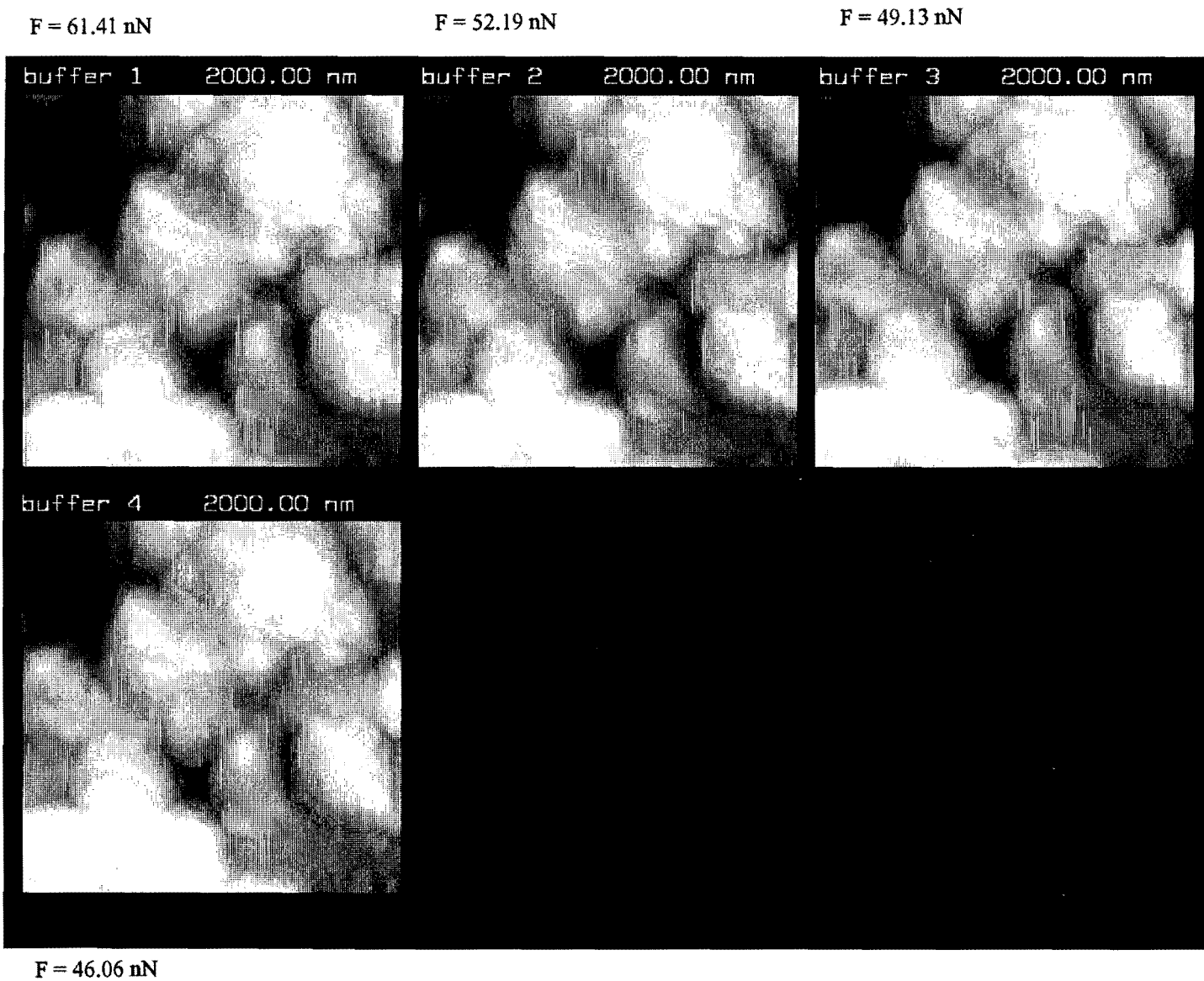
F = 27.89 nN

F = 20.72 nN

F = 30.54 nN

F = 49.63 nN

F = 30.54 nN

buffer 1   2000.00 nm

buffer 2   2000.00 nm

buffer 3   2000.00 nm

buffer 4   2000.00 nm

buffer 5   2000.00 nm

F = 45.81 nN

F = 61.08 nN

buffer 1   2000.00 nm   buffer 2   2000.00 nm   buffer 3   2000.00 nm

buffer 4   2000.00 nm   buffer 5   2000.00 nm   buffer 6   2000.00 nm

F = 50.91 nN   F = 61.09 nN   F = 40.73 nN

F = 61.41 nN   F = 52.19 nN   F = 49.13 nN
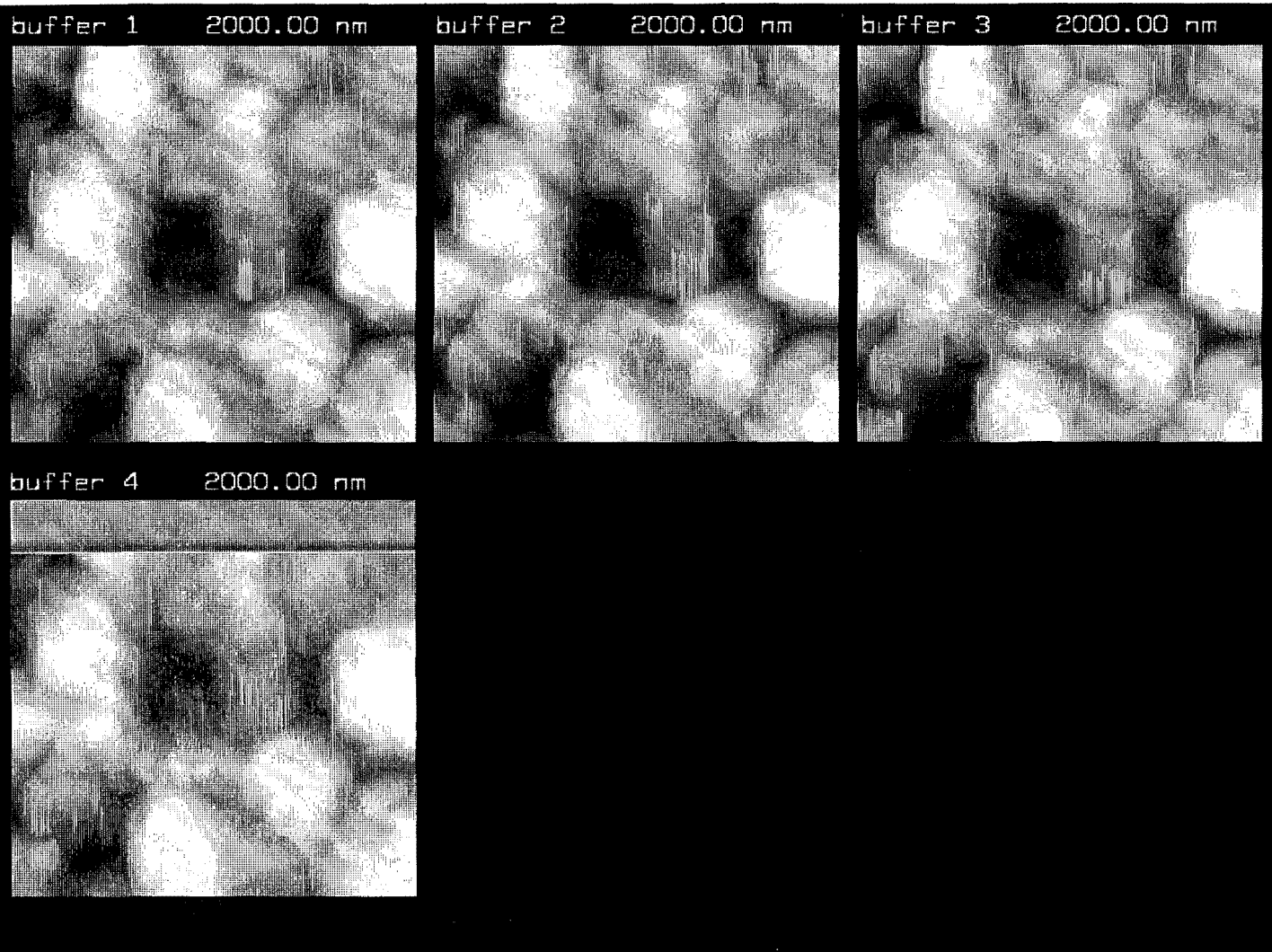

F = 46.06 nN
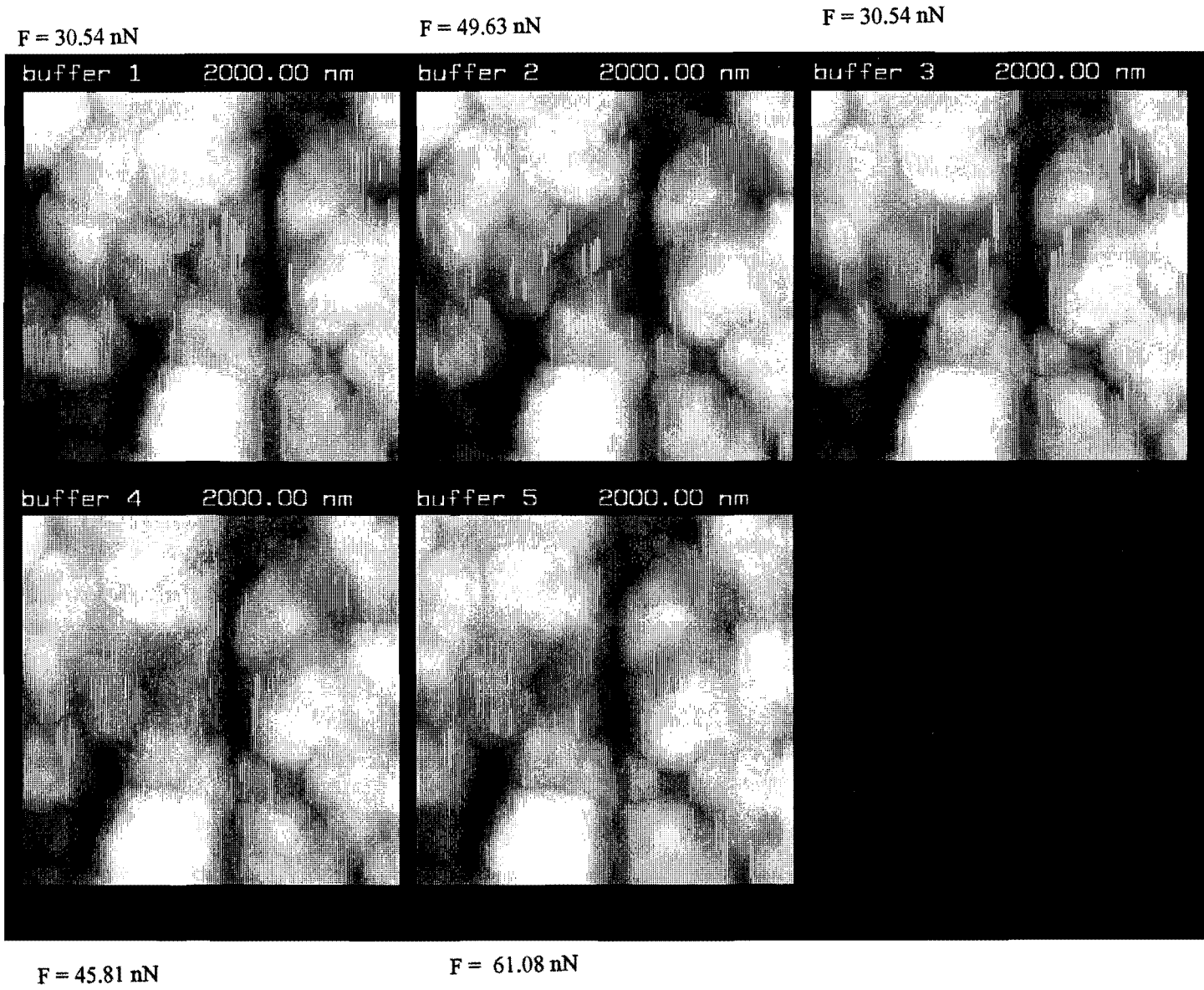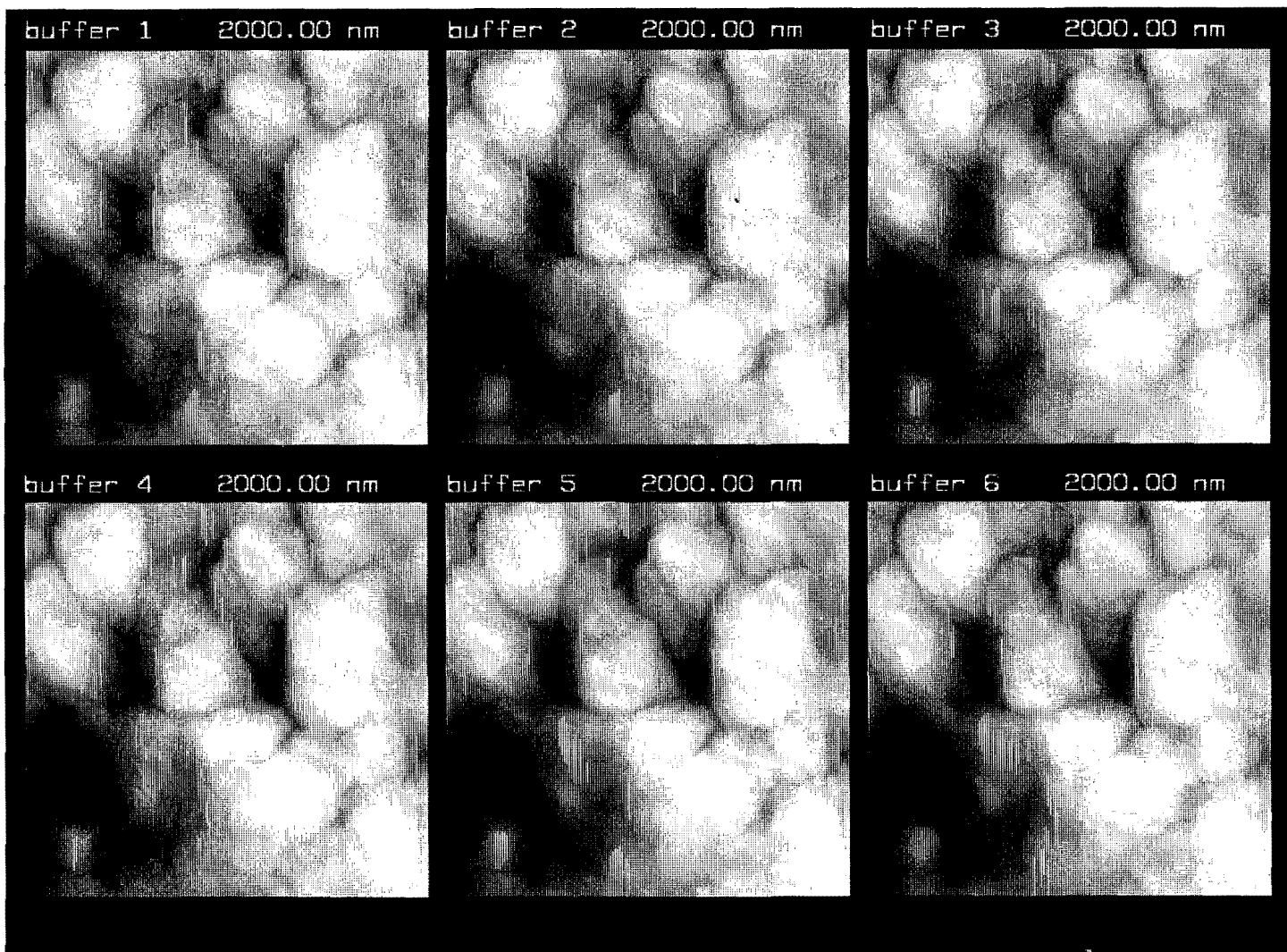
F = 55.37 nN   F = 50.34 nN   F = 40.27 nN

F = 40.27 nN

References

1. A practical guide to scanning probe microscopy, Park scientific Instruments.
2. G. Benedek, Surface Properties of Layered Structures, p.15-21, Kluwer Academic Publishers, Dordrecht, 1992.
3. S.W. Bailey, Reviews in mineralogy, Volume 13, Micas, p.1-17, Bookcrafters Inc, Chelsea, 1984.
4. H. Bengel, H.-J. Cantow, S.N. Magonov, L. Monconduit, M. Evian and M.-H. Whangbo, Surface Science 1994, p.L170-L176, *Tip-force induced surface deformation in the layered commensurate tellurides NbA$_x$Te$_2$ (A=Si, Ge) during atomic force microscopy measurements.*
5. G. Binning, C.F. Quate and Ch. Gerber, Physical Review Letters 1986, p.930-933, *Atomic Force microscopy.*
6. J.P. Cleveland, S. Manne, D. Bocek and P.K. Hansma, Review of Scientific Instruments 1993, p.403-405, *A nondestructive method for determining the spring constant of cantilevers for scanning force microscopy.*
7. Dror Sarid, Scanning force microscopy with applications to electric, magnetic and atomic forces p.181-231, Oxford University Press, New York, 1991.
8. Hecht and Zajac, Optics, p.275-285, Addison-Wesley Publishing Company, Massachusetts, 1976
9. J.Hu, X.-D.Xiao, D.F.Ogletree and M.Salmeron, Surface Science 1995, p.327-358, *Atomic scale friction and wear of mica.*
10. J.L.Hutter and J.Bechhoefer, Journal of Applied Physics, 1993, p.4123-4129, *Manipulation of van der Waals forces to improve image resolution in atomic force microscopy.*
11. Instruction manual Nanoscope II, Digital instruments.
12. C.Julian Chen, Introduction to scanning tunneling microscopy p.1-75, p.171-213, p.313-325, Oxford University Press, New York, 1993.
13. E.M.Lifshitz, Soviet Physics, 1956, p.73-85, *The Theory of Molecular Attractive Forces between Solids.*
14. S. N. Magonov and M.-H. Whangbo, Surface Analysis with STM and AFM, Experimental and Theoretical Aspects of Image Analysis, VCH, Weinheim, 1996
15. G. Meyer and N.M. Amer, Applied Physical Letters, 1990, p.2100-2101, *optical-beam-deflection atomic force microscopy: The NaCl (001) surface.*
16. J.M. Neumeister and W.A. Ducker, Review Scientific Instruments, 1994, p.2527-2531, *Lateral, normal and longitudinal spring constants of atomic force microscopy cantilevers.*
17. S.T. Smith and L.P. Howard, Review Scientific Instruments, 1994, p.903-909, *A precision, low-force balance and its application to atomic force microscope probe calibration.*
18. A. Torii, M. Sasaki, K. Hane and S. Okuma, Measurement Science & Technology 1996, p.179-184, *A method for determining the spring constant of cantilevers for atomic force microscopy.*

19. K.O. van der Werf, C.A.J.Putman, B.G.de Grooth and J.Greve, Appl.Phys.Lett. 1994, 1195, *Adhesion force imaging in air and liquid by adhesion mode atomic force microscopy.*

20. D.E. Williams, The Journal of Chemical Physics, 1967, p.4680-4684, *Nonbonded Potential Parameters Derived from Crystalline Hydrocarbons.*